Republic of IRAQ
Ministry of Higher Education &Scientific Research
Al-Nahrain University /College of Science
Department of Physics

Structural , D.C , and A.C. Mechanism for thermally evaporated Cd_XSe_{1-X} thin films

A THESIS

Submitted to the

Physics Department, College of Science, Al-Nahrain University

In Partial Fulfillment for the Degree of Master of Science in Physics

By

SABA NASHAA`T SAEED
B.Sc. 2005

Supervised By

Dr. Izzat M.Al-Essa
Professor

Dr. Talib S.Hamadi
Lecturer

" بسم الله الرحمن الرحيم "

﴿قـــل هذا من فضل ربي﴾

" صدق الله العلي العظيم "

من الآية (40)

من سورة النمل

Supervisor's Certification

We certify that this thesis was prepared under our supervision at Al -Nahrain University as a partial requirement for the degree of Master of Science in physics.

Signature :
Name : Dr. *Izzat M.Al-Essa*
Title : Professor
Address : Department of physics
College of science,
Baghdad University
Date : / / 2010

Signature :
Name : *Dr. Talib S.Hamadi*
Title : Lecturer
Address : Department of Physics,
College of Science,
Al-Nahrain University.
Date : / / 2010

In view of the available recommendation, I forward this thesis for debate by the examination committee.

Signature:
Name : Dr. Salah A.H. Saleh
Title : Assistant Professor
Address :Head of Physics Department
College of Science,
Al-Nahrain University.
Date : / / 2010

Committee Certification

We certify that we have read the thesis titled **(structural, D.C, and A.C Mechanism for thermally evaporated Cd_XSe_{1-X} thin films)**, as examining committee, and examined the student **(Saba Nashaa't Saeed)** in its contents and found its meets the standard of thesis for the degree of Master of Science in physics.

Signature:
Name: **Dr. Nadir F. Habubi**
Title: Professor
Address: University of Al-Mustansiriyah
Date: / / 2011
(Chairman)

Signature:
Name: **Dr. Emad K. Al-Shakarchi**
Title: Assistant Professor
Address: Al-Nahrain University
Date: / / 2011
(Member)

Signature:
Name: **Dr. Hussien Kh. Al-Lamy**
Title: Assistant Professor
Address: University of Baghdad
Date: / / 2011
(Member)

Signature:
Name: **Dr. Izzat M. Al-Essa**
Title: Professor
Address: University of Baghdad
Date: / / 2011
(Member / Supervisor)

Signature:
Name**: Dr. Talib S. Hamadi**
Title: Lecturer
Address: Al-Nahrain University
Date: / / 2011
(Member / Supervisor)

Approved by University, Committee of Graduate Studies

Signature:
Name: **Dr. Laith Abdul Aziz Al-Ani**
Title: Assistant Professor
Address: Dean of College of science / Al-Nahrain University
Date: / / 2011

الإهداء

إلى من أعتمر قلبه بذكر الله ...

إلى من تحت قدميهما الجنان، من تحملوا أعباء الدراسة معي، من كانوا كالشمس بحرارتها تدفئني، وكالقمربنوره يشع علي، إلى نبض قلبي، نبع الحنان.

أمي وأبي

إلى من كن لطيفات علي وساعدنني في شؤوني لإكمال هذا البحث على أكمل وجه.

أخواتي

إلى من كانوا بصيص الامل الذي أنار نفق علمي.

أساتذتي

إلى المعادن الحقيقية التي لاتظهر إلا في وقت الشدة.

أصدقائي

إلى من ساهم و لو بكلمة علمية أو معنوية لإنجاح هذا البحث ...

أصدقاء النجاح

Acknowledgement

First of all, I thank God for helping me to complete this thesis, and best prayers and peace be unto his best messenger **Mohammed**, his pure descendant, and his noble companions.

I wish to express my deepest gratitude and appreciation to my supervisors ***Prof. Dr. Izzat M.Al-Essa*** **,** and ***Dr. Talib S.Hamadi*** for their guidance, suggestions, support, and encouragement through the research work.

I also would like to express my appreciation to the staff of thin films laboratory especially ***Dr.IssamM.Ibrahim,*** and ***Dr.Kadhim A.El-Wahid*** in physics department of Baghdad University for their assistance.

.

Finally, I would like to express my thanks to ***Areeg A.Hateef*** and to all my friends and to all lovely people who helped me, directly or indirectly to complete this work.

Saba

List of Samples and Abbreviations

Symbol	Description	units
a	Electrode area	cm^2
a.c	Alternative current	Amper
A	Cross section area of the film	cm^2
$\vec{B}$	Magnetic Field	W_b/cm^2
C	Capacitance	Farad
C .B	Conduction Band	
CBH	Correlated barrier hopping	
D^-	Negative Dangling Bond	
D^+	Positive Dangling Bond	
d.c	Direct current	Amper
$d_{(hkl)}$	The Inter Planar Distance for Different Planes	$\overset{0}{A}$
E_a	Electrical Activation Energy	eV
E_c	Conduction Band Energy	eV
E_F	Fermi Level Energy	eV
E_H	Hall Electric Field	
E_v	Valence Band Energy	eV
E_ω	A.C Activation Energy	eV
h	The distance Between The Boat and Substrate	cm
I_o	Direct current	Amper
I_p	Polarization displacement current	Amper
J	Current Density	Amper\cm^2
k_B	Boltzman Constant	J\cm^2
L	Distance between the electrodes	cm
LP	Large polaron Tunneling	
LRO	Long Range Order	
m	Mass of material	gm
$N(E_{ext})$	Density of extended states	cm^{-3}
$N(E_F)$	Density of States Near Fermi Level	cm^{-3}
$N(E_{loc})$	Density of localized states	cm^{-3}
N_A	Acceptors concentration	cm^{-3}
N_D	Donors concentration	cm^{-3}
n	Electron concentration	cm^{-3}
P	Holes Concentration	cm^{-3}
q = e	Charge of Electron	Colomb (C)

QMT	Quantum Mechanical Tunneling	
R	Film resistance	$\Omega.cm^2$
R_H	Hall Coefficient	$cm^2\backslash C$
R_w	Tunneling Distance	$\overset{0}{A}$
r_o	Polaron radius	$\overset{o}{A}$
s	Frequency Exponent	
SP	Small Polaron Tunneling	
SRO	Short Range Order	
T	Absolute Temperature	K
t	Film Thickness	nm
T_a	Annealing Temperature	K
T_s	Substrate Temperature	K
V.B	Valence Band	
V_H	Hall Voltage	Volt
W_m	Maximum Barrier Height	Volt
W_p	Activation enery of polaron	eV
X	Concentration of material	
ΔX	Distance between fringes	$\overset{o}{A}$
x	Width of fringe	$\overset{o}{A}$
XRD	X-Ray Diffraction	
α	polarizability	
ρ	Resistivity	$\Omega.cm$
μ_H	Hall Mobility	$cm^2/V.sec$
$\sigma_{d.c}$	D.C. Conductivity	$(\Omega.cm)^{-1}$
$\sigma_{a.c}$	A.C. Conductivity	$(\Omega.cm)^{-1}$
σ_{tot}	Total conductivity	$(\Omega.cm)^{-1}$
χ'	Real part of susceptibility	
χ''	Imaginary part of susceptibility	
ε	Complex Dielectric Constant	
ε_o	Space dielectric constant	
ε_1	Real Part of Dielectric Constant	
ε_2	Imaginary Part of Dielectric Constant	
ε_s	Static Dielectric Constant	
ε_∞	Dielectric constant at infinite frequency	
ζ	flat distribution	
τ	Relaxation time	sec
τ_D	Deby relaxation time	sec
λ	Wavelength	nm
λ_D	The half peak width of Debye	nm

ρ	Density of materials	cm^{-3}
ω	Angular Frequency	Hz
ω_p	Loss peak frequency	Hz

Abstract

This thesis was including study the effect of different concentration (X=0.1,0.2,0.3,and 0.4), thickness, t (200-500)nm ,and substrate temperature ,T_s (300-393)K on the structural and electrical properties for Cd_XSe_{1-X} thin films ,which prepared by thermal evaporation on glass substrate under vacuum of ($2_t \times 10^{-5}$ mbar), and studying the mechanism of transition for the d.c conductivity and a.c conductivity.

Cd_XSe_{1-X} alloys for different (X) was prepared inside quartz vacuum tube; then heated to melting point and left for five hours to get homogenous compound and then allowed to cool slowly to room temperature. From X-ray diffraction spectrum appeared that all alloys have polycrystalline structure with hexagonal Wurtzite phase at (X=0.2) and mixture phase of hexagonal and cubic at (X=0.1,0.3,0.4).

XRD results shows that all Cd_XSe_{1-X} films for thickness (400 nm) at (T_s=300 K) are polycrystalline with mixture of hexagonal and cubic phase at (X=0.1,0.3,0.4), while the other films at (X=0.2) at the same condition are polycrystalline with cubic structure and the preferred orientation is (111), also it has been found that the structure of the film at (X=0.3), and at room temperature (T_s=300 K) with different thicknesses are polycrystalline with mixture structure a hexagonal and cubic phase and the preferred orientation is (111), but at the same concentration (X=0.3) at thickness (400 nm) with different substrate temperature the films are polycrystalline with hexagonal and cubic structure, and the concentration of Se increases with substrate temperature increasing.

D.C. conductivity showed irregular behavior with increasing concentration (X), but it's increases with the increase in thickness (t), while decrease when increase substrate temperature, and all films have two activation energy.

From studying the variation of A.C. conductivity and the exponent factor (s) with angular frequency and temperature, we founded that the correlated barrier hopping (CBH) is a suitable model to explain experimental result, also by use the Cole-Cole diagram we calculated relaxation time (τ),(τ_D) for ideal and non ideal Debye model respectively , polarization (α), and the static dielectric constant (ε_s) and we found that the static dielectric constant increasing from 3.7 to 28 with increasing the substrate temperature from 300 K to 393 K, but the relaxation time decreasing with increasing the substrate temperature.

Hall measurements confirmed that all the films are (p-type).

List of Contents

Chapter One

Introduction

(1-1) Introduction:

The term of “Thin Films “is used to describe a layer or several layers of the atoms of a certain substance whose thickness ranges between (10nm) and less than (1 μm.)[1]. Being very thin, the film layer deposits on certain plates chosen according to the nature of the study or the scientific need. Such plates could be glass slides, silicon wafers, aluminum, quartz and others. The physical properties of the thin films are different from those of their characteristics materials in their bulk. [2]

These films are first made by (Busen & Grove) in 1852 by using (Chemical Reaction). In 1857, the scientist (Faraday) has been able to obtain a thin metal film by means of (Thermal Evaporation).[3]

The thin films have huge importance today, because their applications industry, these films have been various used that they are used in the field of manufacturing (p-n) junctions, rectifiers, mirrors with two types ordinary and thermally, reflected & anti-reflected coating, computers, photograph, digital photo, integrated circuits, and of optical communications as light emitting diodes, lasers of semiconductors, detectors and of solar cells, ….. , etc.[4]

There are many methods to prepare thin films, as following:[5]

1- Thermal Evaporation.

2- Sputtering.

I- DC sputtering.

II- RF sputtering.

3- Glow Discharge.

4- Molecular Beam Epitaxy(MBE).

5- Chemical Vapor Deposition(CVD).

Thermal evaporation method is used to prepare Cd_XSe_{1-X} films in this research. The deposition by thermal evaporation method is simple, very convenient and most widely for producing thin films. It may be achieved by resistive heating, and this method consists of heating the material with resistivity heated filament of boat by passing electrical current through it in vacuum chamber at pressure between 10^{-5}-10^{-9} Torr. Pressure lower than 10^{-5} Torr are necessary to ensure a stright-line path for most of the emitted vapor atoms[6]. Thin films preparation in thermal evaporation depends on substrate temperature, substrate-source separation and orientation, base gas pressure in the chamber and boat or filament temperature[6]. The rate of deposition of the vapor on a substrate depends on the vapor source geometry, and its position relative to the substrate[7].

(1-2) Semiconductors Materials:

These materials have an electrical conductivity between conductors and insulator materials about (10^3 _ 10^{-8}) $(\Omega.cm)^{-1}$ .There intermediate properties are determined by the crystal structure, bonding characteristics, and electronic energy band.

The crystal structure has a profound effect on the electronic and optical properties of the semiconductor. According to the quantum theory, the energy of an electron in the crystal must fall within well-defined bands. The energy of valence orbital which form bonds between the atoms represent just such a band of states, the valence band .The next higher band is the conduction band that is separated from the valence band by the energy gap, or band gap[8]. The width of the band gap is a very important characteristic of semiconductor and is usually denoted by E_g [9] .

(1- 3) Semiconductors Classification :

Semiconductors classified according to its structure as [8,10]:

1-3-1 Crystalline semiconductor

There are two types of the ordered array of atoms in crystalline semiconductors:

a) Single Crystalline Semiconductors

Single crystal is defined as materials characterized by having atoms arranged in a pattern that is repeated periodical over long distance (Long Range Order [LRO]) as shown in fig (1.1-a).The single crystal semiconductor gives rise to three dimensions (3D) with spot diffraction patterns where the overlap among different diffraction peaks is minimal. Most of semiconductor devices require the used of single crystal material because of its electrical properties are superior to those of a non single crystal semiconductors[11].

b) Polycrystalline Semiconductors

The structure of polycrystalline materials consist of many tiny single crystal known as grains or crystalline which are separated by grain boundaries each of which contains a periodic array of atoms and is considered to pass long range order, while the grain in polycrystalline state posses (Short Range Order [SRO]) with random grain sites, shape and orientation packing as shown in fig (1.1-c) [11].

1-3-2 Amorphous Semiconductors:

Amorphous semiconductor is defined as materials in which the atomic sites are randomly arranged in three-dimensions, as shown in fig(1.1-b).

Amorphous semiconductor is lacking long rang periodic ordering in their lattice network, [i.e. they have short rang order (SRO)] because of the variation in the inter atomic distance and bond angles that mostly form covalently bonded atoms which are arranged in an open network, through its

to bonds are saturated, with correlations in the ordering up to the third or fourth nearest neighbors . The properties of amorphous semiconductor thin films are very sensitive for the preparation technique and thermal history because there is no limit to the variation of bond lengths and angles in addition to the preparation[12].

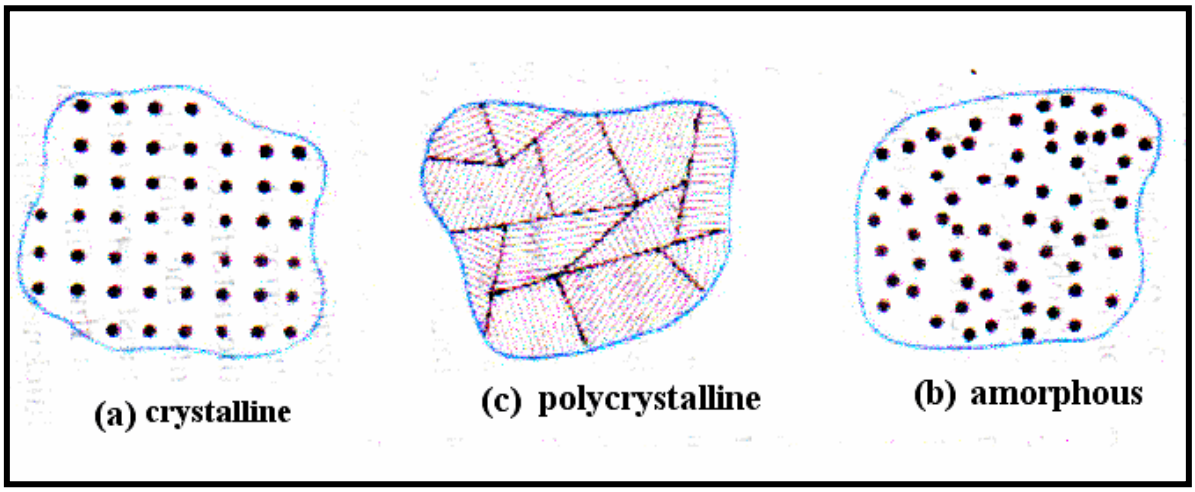

Figure (1.1) : shown structure of solid state[13]

(Alexander 1974)[14] could distinguish the crystalline and amorphous materials by studying the diffraction patterns of these materials ,which caused by dispersed the X-rays ,then he found out that the diffraction patterns of the one-crystalline materials will be spots , while it be wide and dim light rings which overlaps and center joined in the amorphous materials.

The amorphous materials are thermodynamic unstable, at the time when these materials are getting the enough energy transformed to the polycrystalline materials and after that transformed to the crystalline materials.

The critical point of the energy barrier is the limit between the amorphous and crystalline materials, which measured by the atomic measurement, as applying

amount of energy which is enough to change the energy barrier and transformed the amorphous materials to the crystalline materials, as shown in fig (1.2).

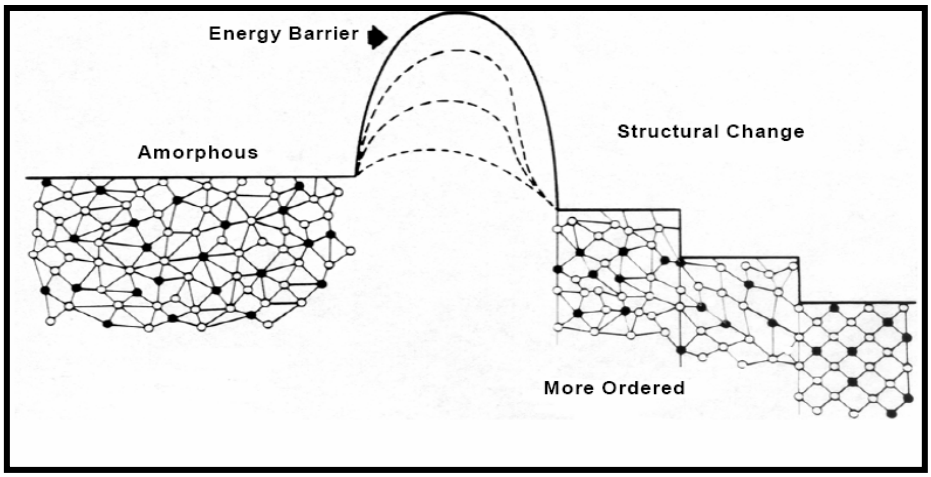

Figure (1.2): structural transformation from amorphous to crystalline.[15]

This transformation of these materials is responsible about the changing of many physical properties,

(1-4) The physical properties of CdSe

Cadmium Selenide **(CdSe)** is a binary chalcogenides (II-VI) semiconductors. The atoms of (Cd) and (Se) have been joined with each other by the covalent bonds, which caused by subscription two electrons between (Cd) and (Se) atoms[16].The (CdSe) compound consider as a toxic black bulk materials[17], which influenced to atmospherically circumstances especially the oxygen[18], hence imperative studying its properties under vacuum As a semiconductor CdSe has a band gap of 1.74 eV at 300 K and a n-type semiconductor which make it an interesting material for various application such as solar cells, thermal detectors and photo detectors[19], also it has been fit for nuclear detectors because of its atomic weight equal (40)[20].

(1-5) Crystallography of (CdSe)

Most of compound semiconductors form the zincblende structure, but a few of (II-VI) compounds crystallize in slightly different form known as wurtizite, in which the tetrahedral bonding is maintained but the two interlocking sub lattices are hexagonal rather than (FCC) .

The lattice structure of CdSe can be found in the forms of sphalerite (cubic) and wurtizite (hexagonal) as shown in figure (1.4-a,b). The former is a metastable phase constituting the almost exclusive product of an electrochemical formation process, while the latter is thermodynamically stable structure obtained either by annealing the cubic phase or directly by various preparation techniques[21].

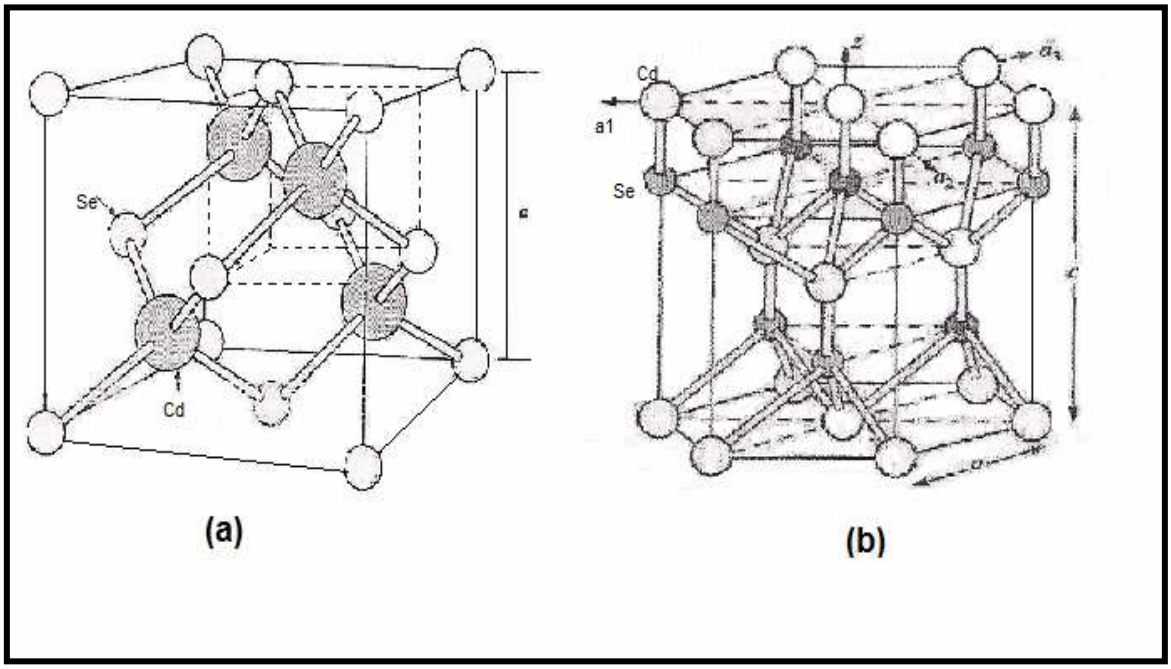

Figure (1.3): the structure of CdSe (a) Zincblende structure (b) Wurtzite structure.[22]

(1-6) Literature Review

Kubovy *et. al* [23], observed that the structure and chemical composition of the CdSe films which evaporated on glass and mica substrate at room temperature are strongly dependent upon the deposition rate (0.2 to 700 $\overset{\circ}{A}/S$) , because at low rate of deposition films with amorphous structure appear, while for medium rate the crystalline size of CdSe increases ,and at high rate the films consist of a Cd – Se phase which is formed by amorphous Se and dispersed Cd.

Snejdar ,and Jerhot. [24], observed that the resistivity of CdSe film increase with increasing the substrate temperature from (298-473) K, while the concentration of carrier decrease.

Thutupalli *et. al* [25], studied the structural properties for CdSe films which deposited at different substrate temperatures (R.T-473)K, he found that the films have a hexagonal structure at room temperature , while the cubic phase appeared when the substrate temperature increased.

Dhere *et. al* [26], reported the structural characterization of CdSe films about (1μm) thick deposited on unheated glass substrates, by the reflection electron diffraction studies showed the growth of a one dimensional [001] texture orientation of the hexagonal phase, and illustrated the resistivity of films decrease by increasing the heat treatment from 0.035(Ω.cm) at room temperature to 0.02 (Ω.cm) at 413 K , and he found that the resistivity increased by increasing the rate of deposition from 0.035 (Ω.cm) at 8.8 ($\overset{0}{A}/S$) to 0.735(Ω.cm) at 79.4($\overset{0}{A}/S$).

Sharma, and Barua [27], found that the electrical resistivity of the CdSe films which prepared by thermal evaporation method, decrease with increasing the substrate temperatures which was attribute to the recreystallization, in addition to the increasing the mobility and decreasing the concentration of charge carrier.

Uthanna , and Reddy [28], pointed to the crystal structure of CdSe films which prepared by thermal evaporation method was polycrystalline and the structure become better by increase the substrate temperature , while all the films were found to be (n-type).

Masahiko ,and Tado [29], prepared the CdSe compound by the molecular beam technique, and the structural examination showed that the films have the hexagonal phase were preferentially oriented with (001), with the grain size increased by increase the substrate temperature from room temperature to 573 K ,and he found that a large value of the electrical resistivity equal ($1*10^5$ Ω.cm) at substrate temperature (473 K).

Raoutl *et. al* [30], noticed that the values of resistivity of the CdSe films which prepared by thermal evaporation method to be unstable, but after annealing it was much order especially at temperature (618 K), because of the improvement of a crystallization by increasing the grain size and discarding from the defect like pending bond and vacancies in the energy gap.[31]

Mondale *et. al* [31], pointed up to all CdSe films were found to be (n-type) and the Hall mobility not influenced by a substrate temperature at the range (390-550)K , while the charge carrier increases from ($4*10^{17}$ cm^{-3}) to ($5*10^{18}$ cm^{-3}) at the same range.

Rao, and Islam [32], studied the structural properties for the CdSe films which prepared by electron beam evaporation at room temperature , and the structural examination showed the crystal structure with cubic phase and the preferred orientation along (111) plane.

Shaharie *et. al* [33], found the crystal structure was polycrystalline for all CdSe films which prepared by the chemical deposition, and the electrical conductivity was {10^{-6} $(\Omega.cm)^{-1}$}, while all the films were found to be (n-type).

Makeeha [34], studied the structural and electrical properties of the CdSe films which prepared by a thermal evaporation method with a thickness of (680 nm) at room temperature, the XRD shows that all the samples were amorphous ,while from the d.c. conductivity measurement she founded that the conductivity was 7.84×10^{-7}(Ω.cm) with two activation energies , and all the films were found to be (n-type).

Abbas [35], studied the effect of the rate of deposition and substrate temperature on the structure and electrical properties for CdSe thin films which prepared by thermal evaporation method with thickness of (360 nm), at different rate of deposition ,and different substrate temperature, the structure of thin films appeared variation in the phase when increasing the rate of deposition. From d.c conductivity measurement he noticed that a large value of conductivity was equal 2.55$(\Omega.cm)^{-1}$ for the films at room temperature and rate deposition $(0.2\ ^{0}\!A/S)$,while a small value was equal $39\times10^{-5}(\Omega.cm)^{-1}$ for the films at (T_s=473 K) and rate deposition $(1.2\ ^{0}\!A/S)$, also he found that all the films have two activation energy, while by studying the a.c conductivity measurement he noticed that a large value of conductivity was equal 6.16×10^{-8} $(\Omega.cm)^{-1}$ for the films at room temperature and rate deposition $(0.6\ ^{0}\!A/S)$,while a small value was equal $7.85\times10^{-10}(\Omega.cm)^{-1}$ for the films at (T_s=473 K) and rate deposition $(1.2\ ^{0}\!A/S)$,also he showed the correlated barrier hopping (CBH) was a suitable model to explain experimental result.

Shreekanthan *et. al* [36], studied the effect of various growth parameters like rate of deposition and deposition temperature for the CdSe films which prepared by thermal evaporation method, and he found that the films which deposited at R.T are cadmium rich with segregated selenium globules. But the deposition temperature (453 K) has been found to yield stoichiometric , homogeneous films, and he found that all the films to be (n-type) with atypical low resistivity of the order of $\{10^{-2}\ (\Omega.cm)^{-1}\}$,and two activation energy 0.34 - 1.86) eV at low and high temperature respectively.

Baban *et. al* [37], studied the structural properties of the CdSe thin films which deposited by thermal evaporation under vacuum on to glass substrates. The XRD showed that the polycrystalline films with hexagonal (002) planes and he found that the crystallites size increases when the substrate temperature and the temperature of the evaporation source are increased.

Suthan *et. al* [38], studied the optical and structural properties of the CdSe thin films which deposited by the physical vapour deposition method of electron beam evaporation (PVD.EBE) technique under pressure of ($5*10^{-5}$ mbar) at substrate temperature (T_s =R.T), and different thickness (710,290,160,120)nm .The deposited films grow in nanocrystalline phase with (002) hexagonal plane orientation. The crystalline size of the particles increases as a result of increasing film thickness, and he found that the band gap value is 1.92 eV .

Elahi, and Ghobadi [39], studied the effect of annealing temperature, annealing time, and deposition time on the structural and electrical properties of CdSe thin films which prepared by chemical bath deposition method (CBD), he found that the Films grew with nanocrystalline cubic phase, and he found that the electrical conductivity in the temperature range of (300-475) K was due to the hopping of carriers between localized states at the Fermi levels.

Haidar [40], studied the structural and electrical properties of CdSe thin films, which prepared by thermal evaporation method on glass substrates under vacuum of (10^{-5} mbar) with different thickness(0.5 , 1 , 1.5 , 2)μm , and rate of deposition ($1.5*10^{-3}$ μm/s) at different annealing temperatures (373, 423 , 473)K , he showed by the XRD that all the films were nearly single crystalline with a hexagonal structure , and the preferentially oriented is (002) , and from the studying the electrical properties of these films he found that the d.c conductivity increased with thickness increasing .there were two activation energies for d.c conductivity, which decreases with increasing of thickness. By the a.c conductivity he found that the films with different thickness consistent with correlated barrier hopping model (CBH), also he pointed to all the films were found to be (n-type) conduction.

(1-7) The Aim of Research Work

We note that progress of research and studies that addressed to study the properties of the A.C. conductivity of the CdSe films, and the affected of the concentrations, thicknesses, and substrate temperature on the D.C. conductivity and Hall measurement are not extensively, as well as the impact of these variables on the dielectric properties .Therefore, we focused in our study the effect of each of the concentration, thickness and substrate temperatures on the A.C. conductivity, D.C. conductivity, dielectric properties , and Hall measurement, As well as, the structural properties of the prepared $Cd_X Se_{1-X}$ films in order to give a comprehensive picture of the behavior of electronic transitions and mechanism of transition.

Chapter Two

The Electrical Properties

(2-1) Introduction

The electrical properties of semiconductors depend on many factors ;(heat, light, magnetic field, and doping), the sensitivity of semiconductor on these factors make it an important material in many scientific and technological applications.

(2-2) D.C-Conductivity

The D.C conductivity in semiconductors depends on the presence of free electrons and free positive holes. At (0K), the valance band is regarded as filled and conduction band is empty.As temperature is raised the free electrons are excited into conduction band, and this leaved behind holes in valance band[41] . The electrical conductivity(σ) is given by Ohm's law

$$J=\sigma E \quad \ldots\ldots\ldots\ldots\ldots\ldots \quad (2\text{-}1)$$

Where J: is the current density.

E: is the electrical field.

$$\sigma = nq\mu \quad \ldots\ldots\ldots\ldots\ldots\ldots..(2\text{-}2)$$

Where n: is the carrier's concentration.

q: is the electron charge.

μ: is the mobility.

The change of electrical conductivity with temperature for most cases of intrinsic semiconductors is given by:

$$\sigma = \sigma_o \exp(-E_a/K_BT) \quad \ldots\ldots\ldots\ldots.. \quad (2\text{-}3)$$

Where:

E_a: is the thermal activation energy

T: is the absolute temperature

K_B: is the Boltzmann constant

$\sigma_{o:}$ is the minimum electrical conductivity at (0K)

Indeed for intrinsic semiconductor $2E_a = E_g$, where the Fermi energy is centered at the middle of the gap, and equation above can be written as [42].

$$\sigma = \sigma_o \exp(-E_g/2K_BT) \ldots\ldots\ldots\ldots\ldots (2\text{-}4)$$

(2-3) A.C. Conductivity

A.C measurements are complementary to D.C measurements and not a substitute for them. Alternative current response as a function of frequency offers valuable additional information about the dynamic response of the system. However the principle strength of ac-studies lies their ability to provide information on the polarization response under the study, from which many deductions may be regarding the physical process involved the ac-conductivity for many materials such as amorphous semiconductors, chalcogenide and crystals increases linearly with frequency and obey the empirical formula[43,44] .

$$\sigma(\omega) = A\omega^s \quad \ldots\ldots\ldots\ldots\ldots\ldots\ldots\ldots\ldots\ldots (2\text{-}5)$$

Where A is multiplicity factor, (s) is exponent factor w is the angular frequency. The value of (s) is less than one if A and s are independent on temperature, but if they are temperature dependent, (s) will equal unity at low temperature[45,46] . The exponent (s) is function of frequency and is determined from the slope of a plot ln $\sigma_{a.c}(\omega)$ versus ln (ω) then:

$$s = d\ln\sigma(\omega)/d\ln(\omega) \ldots\ldots\ldots\ldots (2\text{-}6)$$

Alternating current loss measurements are an important means by which deep defect centers may be studied. They are sensitive to processes in which such centers, or groups of centers develop electron dipole moments under the action of the applied field, and the interactions of the applied field with such a pair can in general be split in to two groups[46,55]:

(a) Resonant Absorption.

Due to the interaction between the two centers, the ground state of the combined system will be split into symmetric and anti-symmetric levels.

Resonant absorption of a photon from the applied field will then occur when the photon energy is equal to the ground state splitting, and the presence of a wide range of atomic environments in an amorphous solid ensures that photon absorption will occur over a wide range of frequencies.

Analysis of this type of process suggests, however, that when the photon energy is less than thermal energy (K_BT), the loss due to resonant processes will vary as (ω^2) which is stronger frequency dependence and will be tend to dominate only at higher frequencies.

(b) Relaxation Processes

These processes events, the exciting field changes the relative environment of apair of centers, and causes transitions between them governed by the intrinsic relaxation time of the pair, τ is given by[46]

$$\tau = \tau_0 \exp(\xi) \ldots\ldots\ldots\ldots (2\text{-}7)$$

Where τ_0 is a constant characteristic relaxation time and ζ has a flat distribution.

Generally there are two physical microscopic relaxation mechanisms:

1) Classical hopping of a carrier over the potential barrier separating two energetically favorable sites in which[46] :

$$\zeta = W/K_BT \text{……. (2-8-a)}$$

2) Phonon – assisted quantum-mechanical tunneling through the barrier separating two equilibrium positions. In which case

$$\zeta = 2\alpha R \text{ …….. (2-8-b)}$$

W: the barrier high separated between two positions.

α: the polarizability.

the ac-conductivity is constant at low frequencies and increases rapidly at higher frequencies this behavior is observed in all amorphous semiconductors, so the total conductivity $\sigma_{tot}(\omega)$ at particular frequency is given by [55,46] :

$$\sigma_{tot}(\omega) = \sigma_{dc} + A\omega^s \text{ ……..(2-9)}$$

Where σ_{dc} is the dc conductivity at zero frequency.

Fig (2.1) reveals the ac- conductivity versus angular frequency (ω), region (a) occurs at a very low frequency which is attributed to electrode polarization .Region (b) is due to the dc conductivity and it is frequency independent. Dispersion (c) is due to high frequency and takes the power low form (ω^s), this dispersion occurs at frequency larger than $(1/\tau)$ (where τ is the relaxation time).

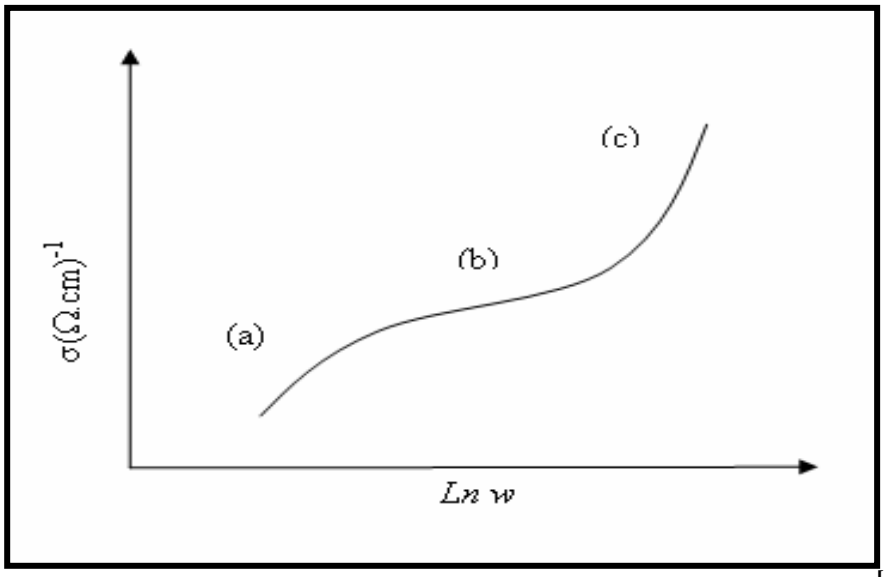

Figure.(2.1) the variation of total conductivity vs. angular frequency[48]

We think that the study of dc and ac - conductivity is very important because it gives a complete picture about the electronic structure of the solid films. According to equation (2-6) $\sigma(\omega)$ dominates at high frequencies or low temperatures while σ_{dc} dominate at low frequencies or high temperatures [47]. It is found that the temperature dependence of $\sigma(\omega)$ is less than that for σ_{dc} ,this means that dc- activation energy is always greater than for ac.

(2-4) Models Of A.C Conductivity

There are several models proposed for ac-conductivity which explain the experimental data for amorphous semiconductors and chalcogenide, these models are briefly reviewed.

2-4-1 Quantum Mechanical Tunneling Model (QMT)

This was the first type of charge transfer process considered first by Pollak[49] and Geballe 1961[49] in connection with impurity conduction in doped crystalline Si . and subsequently applied to the case of amorphous semiconductors first by Austin and Mott (1969)[50].

This model is widely used for deep states within the energy gap (closed to the Fermi level)[44].

The ac conductivity for (QMT) is given by:

$$\sigma(\omega) = Ce^2 k_B T/\alpha N^2(E_f)\ \omega R^4{}_\omega \ldots\ldots\ldots\ldots(2\text{-}10)$$

Where C is a constant and equal to ($\pi^4/24$ or $\pi^2/12$), $N(E_f)$ is the density of states at the Fermi level ($ev^{-1}.cm^{-3}$) and $N = K_B T\, N(E_f)$, is the number of states actually contributing to the a.c loss R_ω is the tunneling distance and given by:

$$R_\omega = 1/2\alpha\ ln(1/\omega\tau_0) \ldots\ldots\ldots\ldots(2\text{-}11)$$

α : is the decay of localized wave function. The exponent (s) of this model given by

$$s = 1 - 4/\ln(\omega\tau_0) \quad \ldots\ldots(2\text{-}12)$$

Where τ_o is the relaxation time.

Note that in this model the exponent (s) is temperature independent but it is frequency dependent and decreases with increasing frequency.

In this model there is no lattice distortion associated with the carrier whose motion gives rise to the a.c conductivity (i.e polaron formation is not considered).

2-4-2 Small Polaron Tunneling (SP)

When addition of charge carrier to the covalent solid causes a large degree of Local lattice distortion; this may form small polaron have total energy (electronic+ distortion) of the system is lowered by an amount (W_P), the polaron energy. As the name implies small polarons are generally assumed to be so localized that their distortion clouds do not overlap. In this case the activation energy for polaron transfer, $W_H \approx (1/2)\ W_P$, and the relaxation time for small polaron tunneling take two formulas according to the temperatures;

at high temperature can be written

as: $\tau = \tau_o \exp(W_H/K_BT) \exp(2\alpha R)$……..(2-13)

Whereas at very low temperatures the relaxation time are no longer thermally activated and can be written as:

$$\tau = \tau_o \exp(W_H/\frac{1}{2}\hbar\omega_o) \exp(2\alpha R)\text{…….(2-14)}$$

Where ω_o the vibrational frequency describing the lattice distortion.

So the ac-conductivity in the high temperature limit expected for the tunneling of the carriers trapped at structural defects.

The frequency exponent (s) may be written as:

$$S=1-4/[\ln(1/\omega\tau_o)-(w_H/K_BT)] \quad \text{....…….. (2-15)}$$

Equation (2-15) predicts that (s) increases as (T) increases and decreases at ω increases as shown in fig(2.3).

2-4-3 Large Polaron Tunneling (LP)

In this model, a.c conductivity occurs by forming an extended polaron which is large compared with the interatomic distance; therefore; it is called large polaron , and the a.c conductivity is given by [46]

$$\sigma_{a.c}(\omega) = (\pi^4/12)\, q^2 (K_BT)^2\, N^2(E_f)\left[\frac{\omega R^4_\omega}{2\alpha K_B T + W_{H_o} r_o / R^2_\omega}\right]\text{…..(2-16)}$$

Where r_o is the polaron radius, and W_{H0} is a function of atomic position.

The frequency exponent s can then be evaluated as

$$S=1-\frac{1}{R'_\omega}\left[\frac{4+6W_{H_o} r'_o / K_BTR'^2_\omega}{(1+W_{H_o} r'_o / K_BTR'^2_\omega)^2}\right]\text{……..(2-17)}$$

Where the reduced quantities $\acute{R}_{\omega}=2\alpha R_{\omega}$ and $\acute{r}_o=2\ \alpha\ r_o$

Where R_{ω} is the tunneling distance .

And the relaxation time for a large polaron tunneling transition is the same of the small polaron at the high temperature in equation(2-13)

From equation(2-17) this overlapping polaron model predicts that s should be both temperature and frequency-dependent.

2-4-4 Correlated Barrier Hopping Model (CBH)

Primarily this mechanism had been first explained by Pike [49].Elliot [46] followed Pike and developed a new model for ac conduction for Chalcogenide material based on Pick's concepts as Correlated Barrier Hopping (CBH), in this model the electrons hopping over the potential barriers between two sites See fig.(2.2) each having a coulombic potential well associated with it. For neighboring sites at a separation R ,the coulomb wells overlap resulting in a lowering of the effective barrier from W_m to a value W ,which for the case of a single electron hopping between positive defect centers,

then the potential barrier will be reduced by the coulomb interaction.

$$W=W_m-\frac{e^2}{\pi\varepsilon\varepsilon_o R} \quad \text{.....(2-18)}$$

Where ε :dielectric constant.

The relaxation time for the electrons to hop over a barrier of height W is given by:

$$\tau=\tau_{\circ}\exp\left(\frac{W}{K_B T}\right) \quad \text{.....(2-19)}$$

so the conductivity is given approximately as:

$$\sigma(\omega)=\frac{1}{6}\pi^3 N^2 \varepsilon\varepsilon_o \omega R^6_\omega \ldots\ldots\ldots(2\text{-}21)$$

Where the hopping distance at a frequency ω is given by:

$$R_\omega = \frac{e^2}{\pi\varepsilon\varepsilon_o[W_M - K_B T \ln(1/\omega\tau_o)]} \ldots\ldots\ldots(2\text{-}22)$$

The frequency dependence in the CBH model (for both limits) can be expressed in terms of the frequency exponent (s):

$$S = 1 - \frac{6K_B T}{W_M - K_B T \ln(1/\omega\tau_o)} \ldots\ldots(2\text{-}23)$$

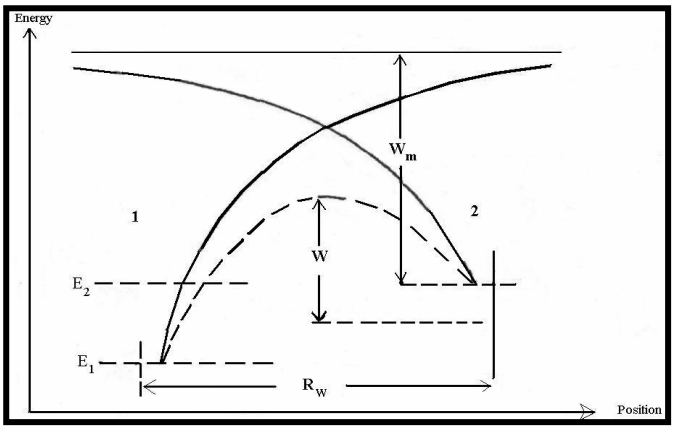

Figure(2.2) Two level system with Coulomb like potential of the barrier height separated between two charge carriers in case of (CBH) [55].

Note that (s) is predicted to be both frequency and temperature dependent.

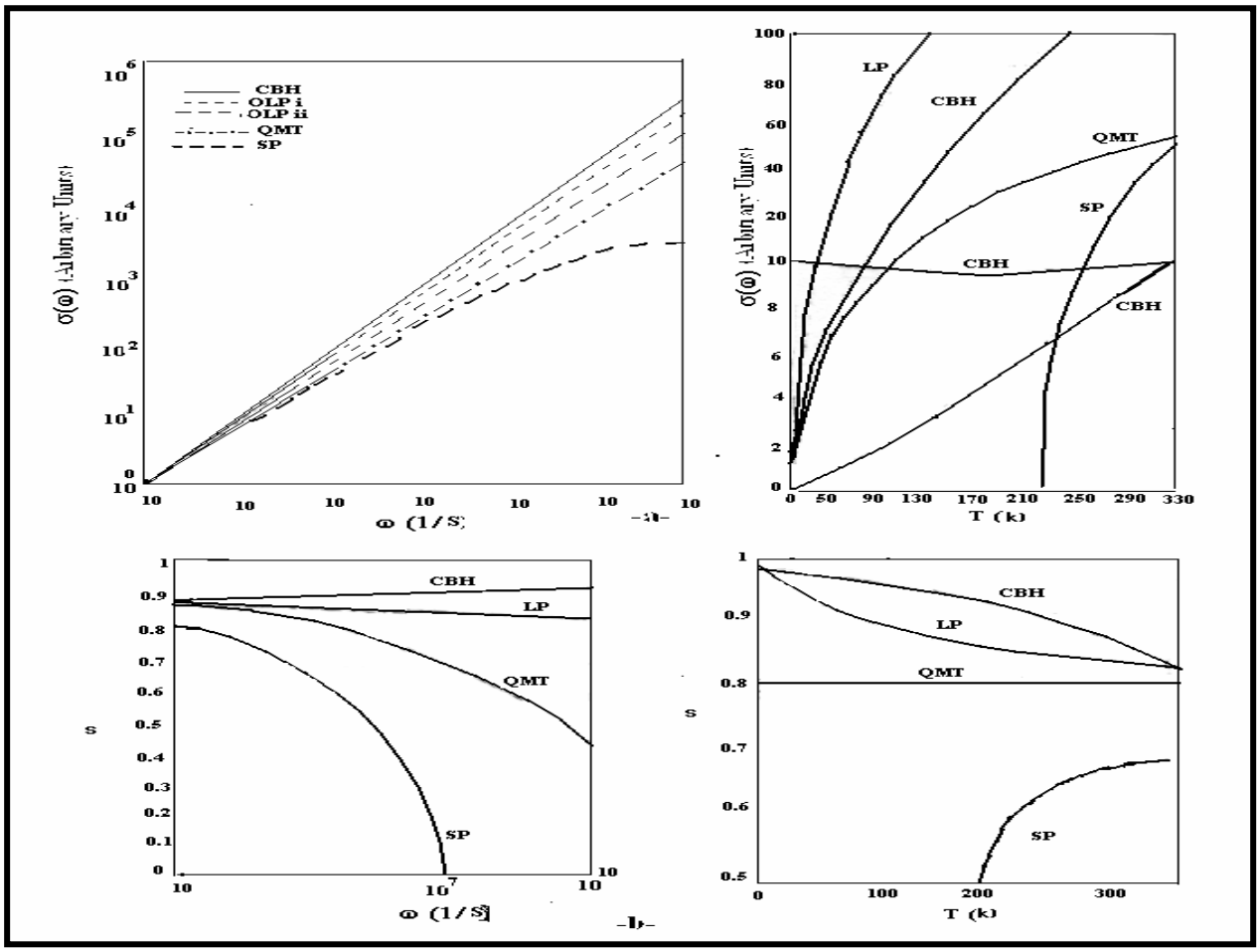

Figure (2.3) a-frequency dependence of exponent *(s)*. b- Temperature dependence of exponent *(s)* in case of CBH, QMT, SP&LP.[46]

(2-5) Polarization and Dielectric Response:

When an external electric field is applied to any material medium, a finite amount of charge transport by either electrons or ions takes place resulting in a direct current I_o and polarization displacement current I_p , the magnitudes of I_o and I_p may vary in wide limits according to the nature of the material medium. The material medium is said to be insulator if the magnitude of I_o is found to be very small in comparison to I_p and in such materials the phenomena of polarization and relaxation dominate , whereas if I_o dominates, the medium is said to be a conductor of electricity.

When a bounded charge or a dipole displaces from its equilibrium position by the application of the applied field, polarization is said to occur . There are several distinct physical mechanisms of polarization which are characterized by very different response rate and are given below[51,52]:

1- Electronic polarization:

A dielectric medium consists of ions surrounded by the electron cloud and posses a complete neutrality in the absence of an external applied field and shows a relative shift in their charge centers when an external field is applied. This shift of electronic charge nature is referred as electronic polarization .As the electrons are very light they have a rapid response to the field changes.

2- Ionic polarization:

In ionic materials, (e.g. alkali halide), the external applied field displaces the ions with respect to each other and induces ionic polarization which has a response time of order (10^{-13} sec), the vibration time of ions.

3- Molecular polarization:

Bonds between atoms in molecules are stretched by the applied of electronic field when the lattices are charged. Small deformation of the ionic bond will increase the dipole moment of the lattice. The polarization achieved in this way is known as molecular polarization.

4- Orientational polarization:

When the molecules of gases or liquids having permanent or induced dipole moments move in line with the applied field, the polarization is said to occur and is termed as orientational polarization.

Basically the mechanisms of electronic, ionic and orientational polarization are due to charges which are locally bound in atoms, in molecules or in the structure of solids. Some mobile charges either electros or ions can also be found in dielectrics and may move by hopping between localized sites. If the hopping is confined only to limited paths it does not produce d.c conduction

which requires transfer of charge from one electrode to other. When a time dependent electric field is applied to a dielectric medium, it disturbs the equilibrium of the dielectric medium, the process of recovery of the equilibrium within the

System after the removal of the disturbing field is called relaxation time.

The first relaxation model was proposed by Debye dealing with the non-interacting permanent dipoles embedded in a viscous medium. So the polarization vanishes by vanishing the applied electric field.

And the response mechanisms of the medium at the limiting frequency range according to Debye model is:

$$\chi(\omega) = \chi'(\omega) - i\chi''(\omega)$$
$$\chi(\omega) = \chi(0)(1 + i\omega\tau)^{-1} \quad \text{.....(2-24)}$$

$\chi(0)$ is the magnitude of the real part of the complex susceptibility at zero frequency, the real and imaginary part of the susceptibility gives by :

$$\chi'(\omega) = \chi(0)\left(1 + \omega^2\tau^2\right)^{-1} \quad \text{.....(2-25-a)}$$

$$\chi''(\omega) = \chi(0)\left(1 + \omega^2\tau^2\right)^{-1}\omega\tau \quad \text{.....(2-25-b)}$$

The ratio of the imaginary part to the real part of the complex susceptibility for a Debye system is given as:

$$\frac{\chi''(\omega)}{\chi'(\omega)} = \omega\tau \quad \text{.....(2-26)}$$

Which is a frequency dependent parameter.

A Debye system is shown in figure(2.4),the dielectric loss curve is symmetric about the loss peak frequency in the logarithmic frequency plot with the characteristic full width at half height as(1.44 decades).

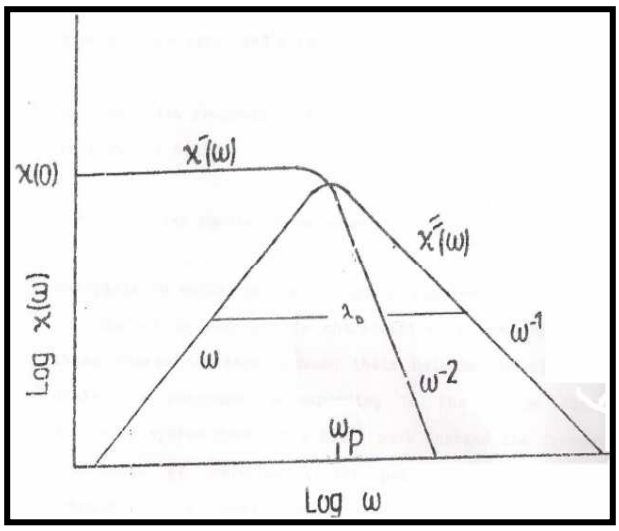

Figure (2.4): The frequency dependence of the real and imaginary components of the complex susceptibility corresponding to the ideal Debye response[52].

In the Debye process the dielectric process is thermally activated by an activation energy E , the loss peak moves towards the higher frequencies with the increase of temperature.

The loss peak frequency w_p can be given as:

$$\omega_p = \frac{1}{\tau} = \omega_0 \exp\left(-E \diagup K_B T\right) \quad \text{.....(2-27)}$$

Where w_0 is the pre exponential factor.

The well known method of displaying Debye type relaxation is by drawing a Cole-Cole plot, Cole and Cole suggested that the real part of dielectric constant ε_1 as a function of imaginary part of dielectric constant ε_2 gives important information about the distribution of relaxation times. In this model the dielectric constant depends mainly on four parameters, the static dielectric constant ε_s, the dielectric constant at infinite frequency ε_∞ the relaxation time τ_D[53], as shown in figure(2.5,a,b):

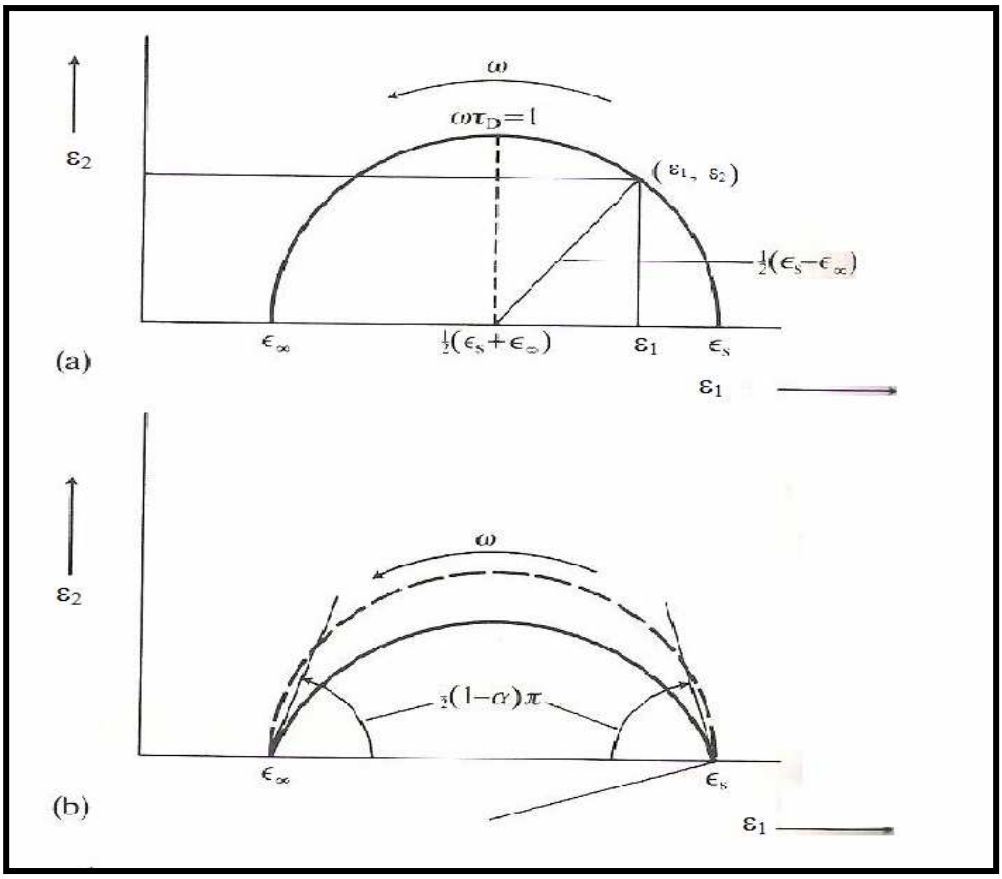

Figure (2.5):a- The Cole-Cole plot for the ideal Debye dielectric.
b- The Cole –Cole plot for the non ideal Deby dielectric. [54]

The simplest plot is for ideal Debye, because which verifies that the locus of the points [$\varepsilon_1(\omega)$, $\varepsilon_2(\omega)$] is a semicircle with radius $\left(\varepsilon_s - \varepsilon_\infty / 2\right)$ .and centre on ε_1 axis at $\varepsilon_1(\omega) = \left(\varepsilon_s + \varepsilon_\infty / 2\right)$.The maximum value of ε_2 occurs when $\varepsilon_1(\omega) = \left(\varepsilon_s + \varepsilon_\infty / 2\right)$this is when ($\omega\,\tau_D$=1) as will be seen in figure(2.5,a), for a Debye dielectric the relaxation time τ_D can be determined by measuring the angular frequency at which ε_2 is a maximum. In the case the centre of a circular arc lies below the horizontal axis, the plot is symmetrical about the

vertical line through the point $\varepsilon_1(\omega) = \left(\varepsilon_s + \varepsilon_\infty / 2\right)$ when ε_2 is a maximum at frequency $[\, 2\pi\tau_o (1+ 2\sin\pi\alpha\,)]^{-1}$ .The circular arc intersect the ε_1 axis at the acute angle of $(1-\alpha)\pi/2$ at both ends as illustrated in figure(2.5,b), where α : the polarizability.

Chapter Three

Experimental Part

(3-1) Introduction

This chapter includes the preparation and processing of Cd_XSe_{1-X} alloy and technique employed to produce Cd_XSe_{1-X} films of various concentrations , (X= 0.1 , 0.2 , 0.3 , 0.4) ,thicknesses and substrate temperature ,which deposited onto glass substrates. The $Cd_X Se_{1-X}$ alloys prepared by us were used as a source to prepare the films.

The X-ray diffraction technique was used to determine the crystalline structure. The electrical measurements (D.C conductivity, Hall effect , and A.C conductivity) were made for films deposited on glass substrates to study the transmissions mechanisms and there models in addition to study the dielectrics responsibility .

All these procedures are illustrated as scheme in fig (3.1).

(3-2) Cd_XSe_{1-X} Compound preparation

The Cd_XSe_{1-X} with (X=0.1, 0.2, 0.3, 0.4) compound were prepared as alloys by using stoichiometric and high purity (99,999%) cadmium metal and high purity (99,999%) selenium metal obtained from Balzeres company. Each element weighted according to its atomic weight and then mixing in quartz tube (length=7 cm, diameter=0.9 cm) evacuated at pressure of (10^{-3} mbar).

The tube was sealed and heated in electrical program controller furnace of type (Qallenhamp),England , at temperature(925 K), and maintained at this temperature for about two hours and then raised to (1173 k),and also maintained at this temperature for about two hours and then allowed to cool slowly to room temperature as shown in fig (3.2)

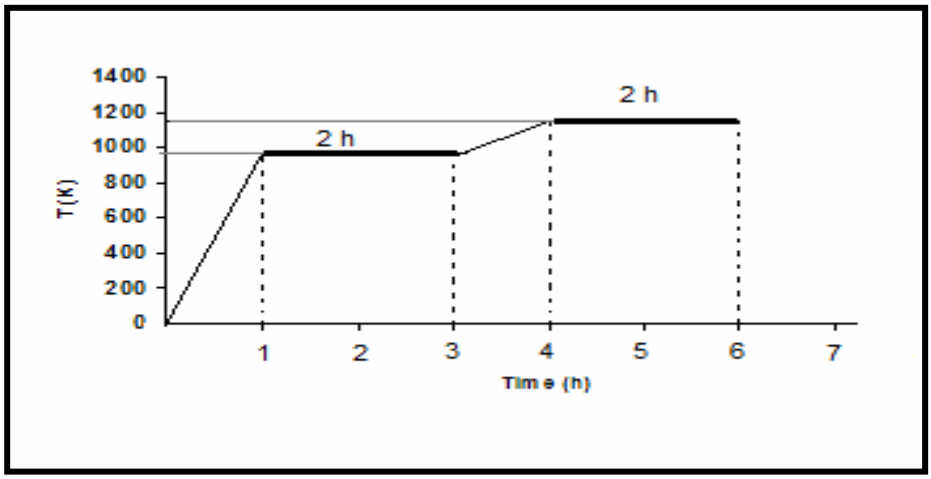

Figure (3.2) The curve of preparing Cd $_X$Se$_{1-X}$ alloy

After that the ampoule was broken and the prepared compound of Cd_XSe_{1-X} was taken out and powdered to grain powder for examined by X-ray diffraction to be sure of the purity and structure of the compound. The powder of the compounds was used as a source of the of the evaporation to prepare the films.

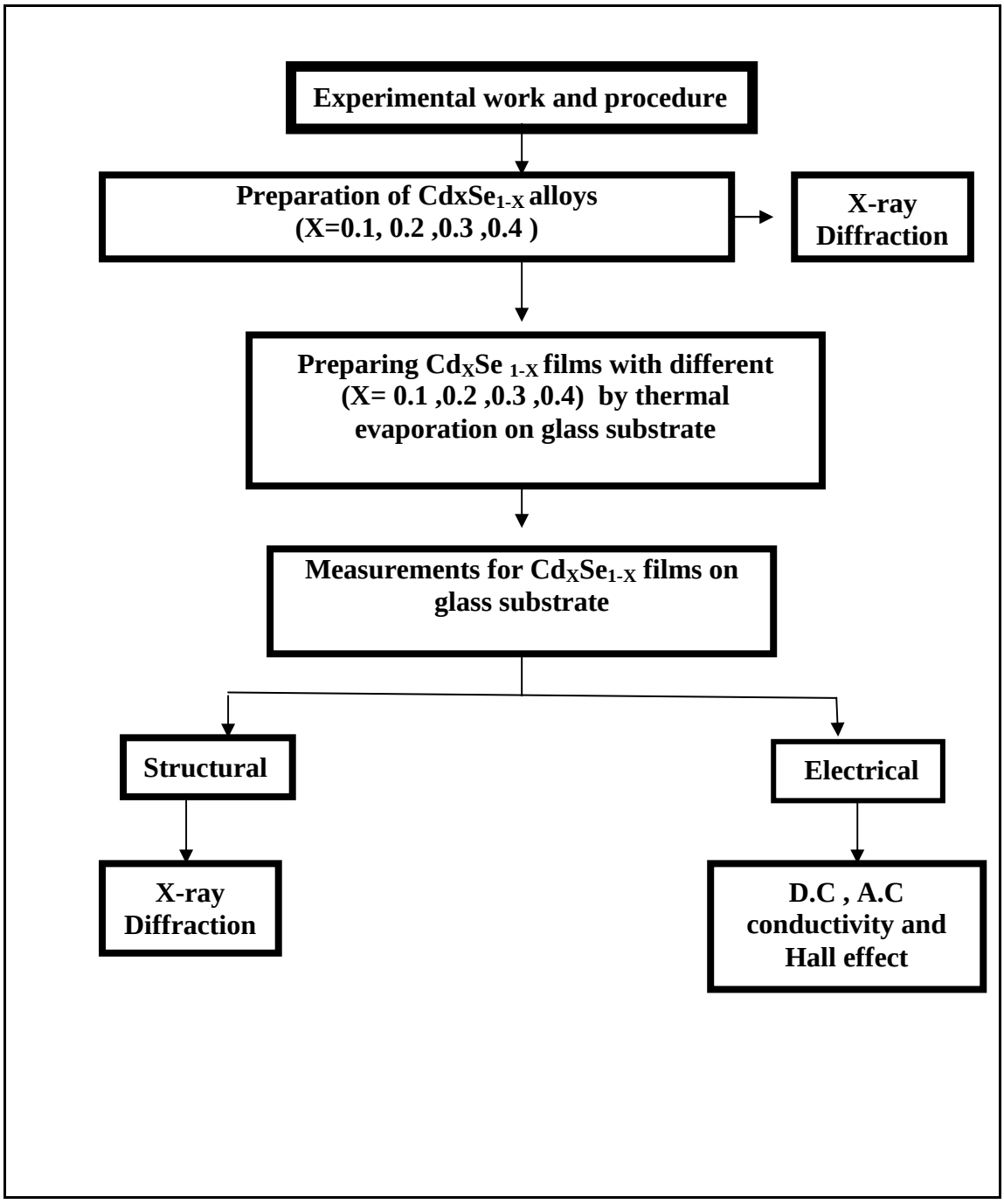

Figure(3.1) Schematic diagram for the experimental work.

(3-3) Masks

The mask is a piece of aluminum foil having thickness (0.2 mm) With the same size of substrate. Various shapes of masks were used to determine the shape of films and electrodes for different measurement as shown in fig (3.3)

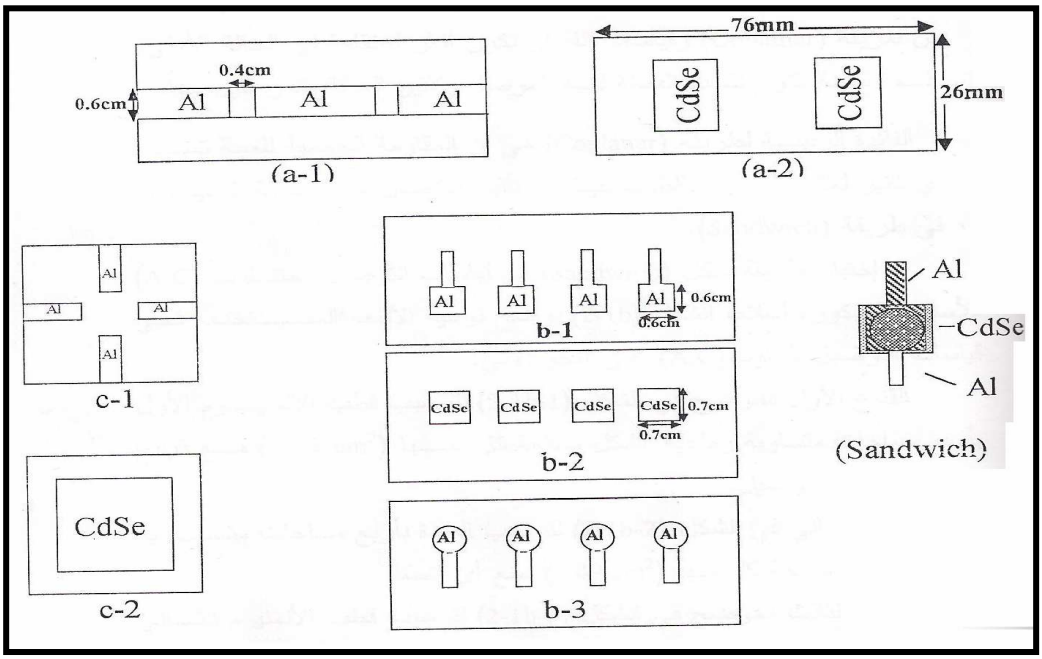

Figure (3.3) The masks with solid lines represent a) D.C mask Measurement b) A.C mask Measurement c) Hall Effect mask Measurement

Thin films can be prepared in sandwich or coplanar geometries according to the type of the measurements ,fig(3.3a) shows that the coplanar geometry has been used for D.C conductivity measurements ,and fig(3.3b) shows that the sandwich geometry has been used for A.C conductivity measurements.

The sandwich techniques have a number of important advantages[55]:

1- The conductance of the sandwich sample is generally much higher than the possible in coplanar geometry, and the loss measurement more straight forward.
2- The sample capacitance is dominated by the active semiconducting region as edge effects are small.

The main advantage of using coplanar techniques is that the bulk resistance of the sample generally masks any contact effects. Contact effects are the major problem associated with sandwich geometry.

The masks were cleaned according to the following stages:

1- Washed in distilled water.
2- Immersed in a pure alcohol.
3- Dried by blowing..

(3-4) substrate cleaning

The type and nature of the substrate are the influence parameters, the substrate ideally should has no chemical reaction and can not change the properties of the film except for sufficient adhesion. The Cd_XSe_{1-X} films were deposited on glass substrates (type corning, Germany) with dimensions (7.6 x2.6 x0.1) cm .

The cleaning procedure of the substrates could be summarized as follows:

1- They were cleaned by using detergent water to remove any oil or dust that might be attached to the surface of the substrate, and then they were rubbed gently under tap (15) minutes.
2- After that, they were placed in a clean beaker containing distilled water and then rinsed in ultrasonic unit for (15) minutes.

3- Step(2) was repeated by replacing the distilled water with pure alcohol solution.

4- The slides eventually were dried by air blowing and wiped with soft paper

(3-5) The specification of Boat

The evaporation method requires using a boat or filament of tungsten (W) and molybdenum (Mo) as sample evaporation source, the suitable boat must posses high melting point and should not react with the evaporation material.

The design and shape of the boat must also be selected . To evaporated the aluminum electrodes a basket or spiral filament of tungsten (W) of (3683 K) melting point was used, as shown in fig (3.4 a) .A molybdenum boat (Mo) with Baffle to prevent material sputtering during evaporation process of (2895 K) melting point was used to evaporate (Cd_XSe_{1-X}) films, as shown in fig (3.4b). The current was passed through the boat in order to clean it and drive off the surface contamination. The temperature that was produced from the current should be below the melting point of the boat material.

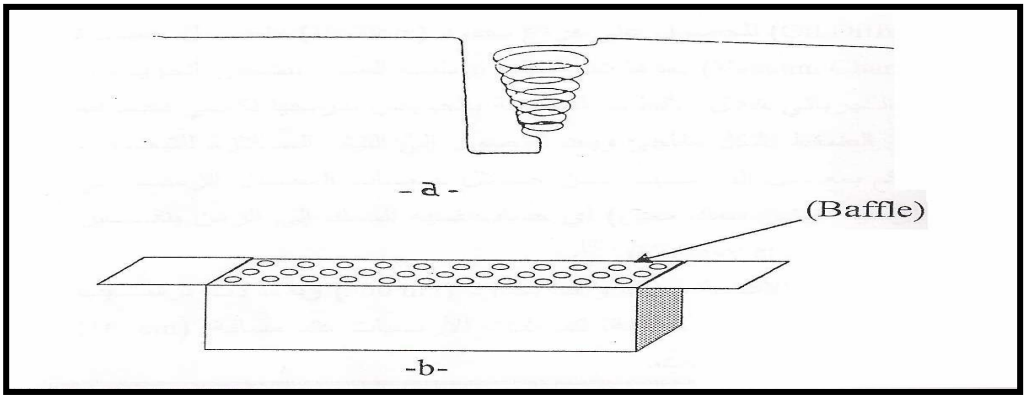

Figure (3.4) Types and shapes of, (a)Tungsten spiral boat, (b) Molybdenum boat

(3-6) Vacuum Technique

The vacuum unit system, which is used to prepare thermally evaporated Cd_XSe_{1-X} films, was Edwaed coating unit model (306 A). The vacuum consist of three main important parts, the vacuum enclosure (chamber),the rotary pump which represents the first stage of vacuum technique called roughing stage and would provide the pressure in the chamber to about (10^{-2} mbar), while the diffusion pump which represents the second stage, called the high vacuum stage by which the pressure decreases to about (4×10^{-5} mbar).

The main construction of the vacuum unit is shown in fig(3.5)

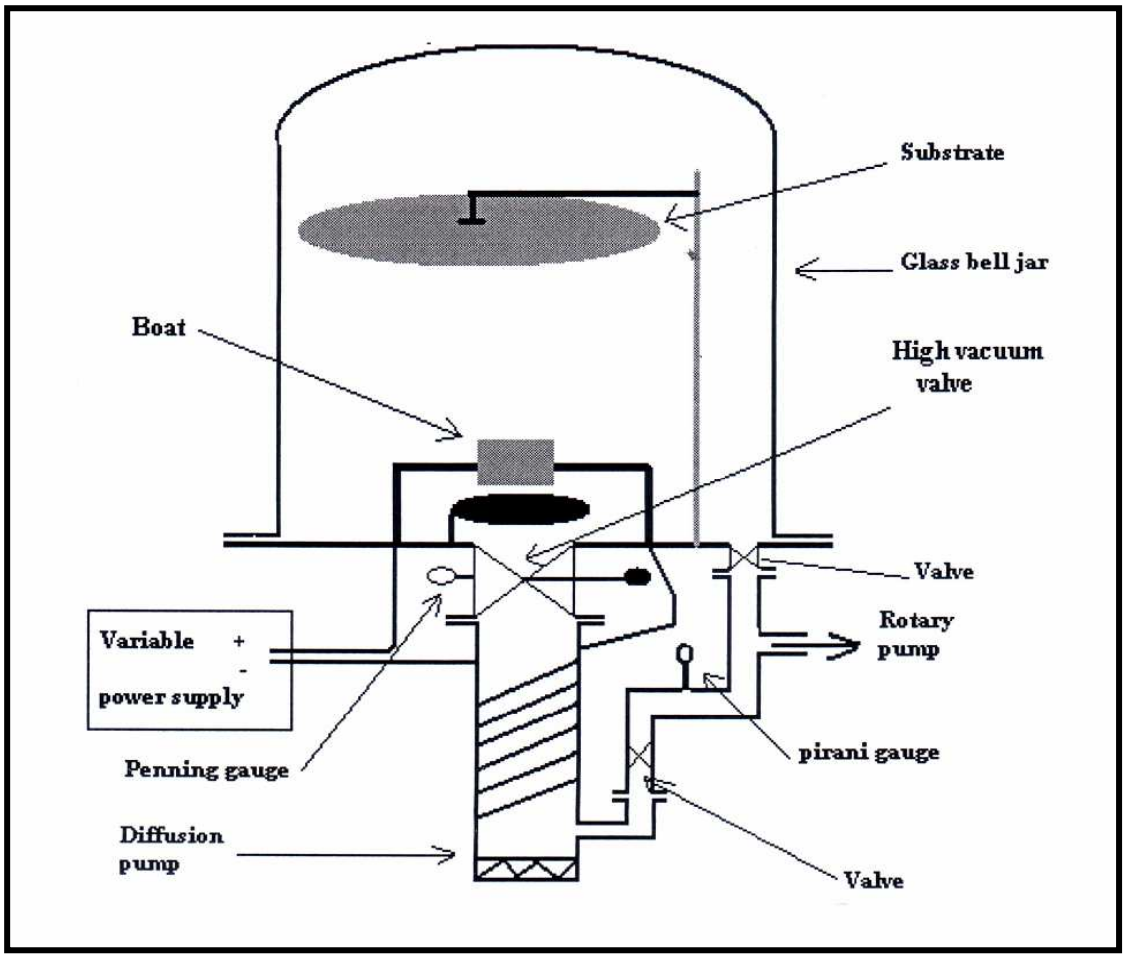

Figure (3.5): Typical experimental set up of thermal evaporation system .

The substrates were fixed on a spherical holder and placed in position at height of about (15 cm) above the boat. When the system is pumped down to a vacuum of (10^{-5} mbar), an electric current was passed through the boat gradually to prevent breaking the boat , when the boat temperature reached the required temperature the deposition process starts. After these two steps the current supply was switched off and the samples were left in the high vacuum for one day, and then the air was admitted to the chamber then the films were taken out from this coating unit, and kept in the desiccator until the measurements were made.

The films of Cd_XSe_{1-X} of different concentrations (X=0.1, 0.2, 0.3, 0.4) were deposited at thickness (t=400 nm) and substrate temperature (T_s=R.T) while the films of Cd_XSe_{1-X} at (x=0.3) was deposited at different thickness (t=500, 300, 200)nm and different substrate temperature (T_s =348,373,393) K.

(3-7) Thickness Measurements:

Vacuum deposited films used for electrical, optical or other purposes must normally be deposited to a specified thickness. The thickness methods are:-

3-7-1 Weighting Method:

A given film thickness may be obtained by the simple formula :

$$t=m/2\rho\pi h^2 \quad \ldots\ldots\ldots\ldots\ldots\ldots(3\text{-}1)$$

Where t=is the film thickness

m =is the mass of the materials to be evaporated.

h = is the source (boat) to substrate distance .

ρ = is the density of materials to be evaporated.

As shown in fig (3.6)

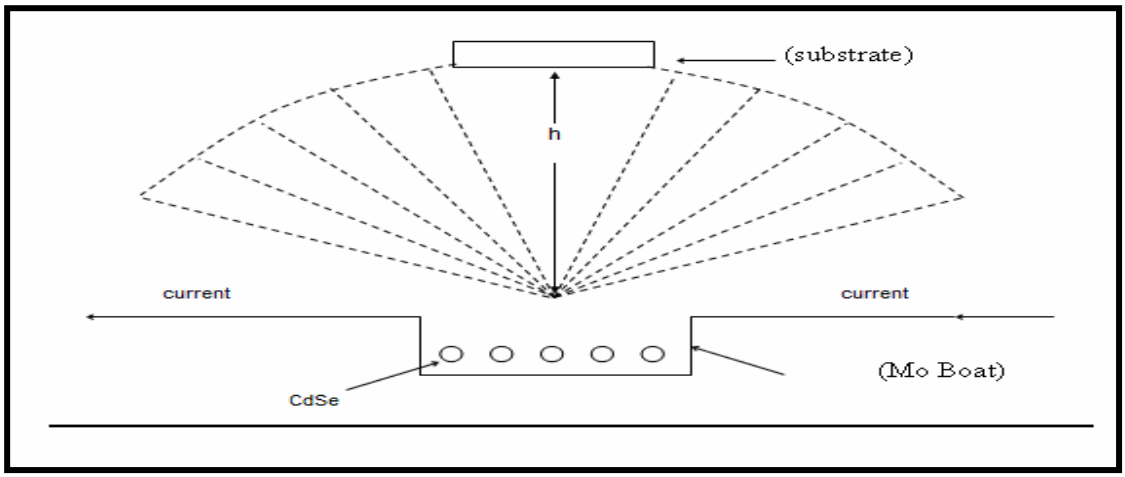

Figure (3.6) The idea of weighting method.

This method gives an estimate of the deposited films thickness that is safe to work with. The error percentage in this method is 30%.

3-7-2 Optical Interference Fringes:

Wiener (1887) was the first to measure the thickness of the films using optical interference fringes. His method is an application of Fizeau fringes of equal spacing. Donaldson and khamasavi used the multiple beam interferometric method for precise measurement of film thickness. Tolansky(1948) has given detailed attention to the various factors influencing fringe width and for the production of sharpened multiple beam Fizeau fringes[56].The following conditions must be cosidered

1- The surface must be coated with high reflecting films
2- The film must be of uniform thickness.
3- The air gap between the flat and specimen surface must be as small as possible (less than 0.01mm)
4- The incidence beam should be normal.

Fizeau fringes of equal thickness are obtained in an optical aperture of the type shown in fig.(3.7) the film thickness(t) is given by:

$$t = \frac{\lambda}{2}.\frac{\Delta x}{x} \quad \ldots\ldots\ldots\ldots\ldots\ldots(3\text{-}2)$$

Where Δx is the shift between the interference fringes, x is the distance between the interference fringes and λ is the Na wavelength (5893 **Å**).

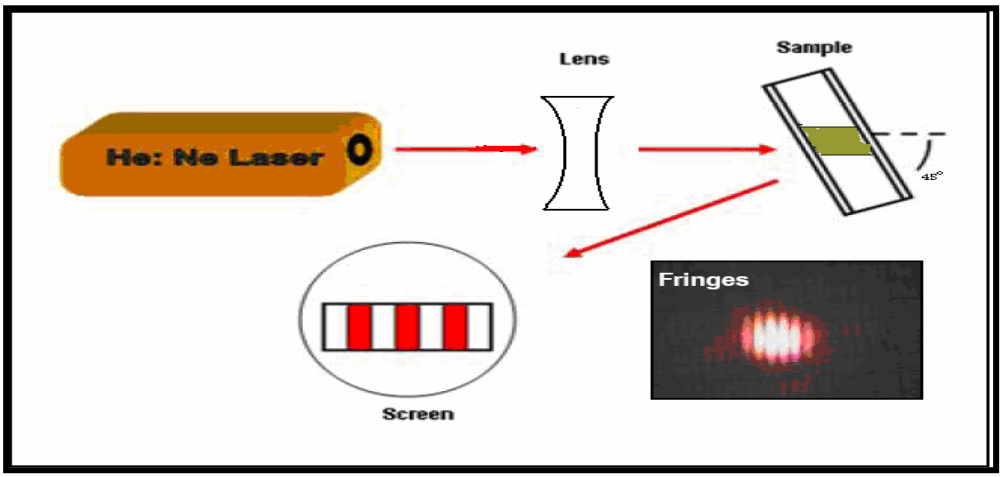

Figure (3.7): The schematic diagram of the film thickness measurement.

(3-8) X-Ray Diffraction Measurements:

The structure of the Cd_XSe_{1-X} films grown on glass substrates with different (X), substrate temperatures and thickness have been examined by X-ray diffractions using a Philips X-ray diffractometer system which records the intensity as a function of Bragg's angle. The source of radiation was Cu(k_α) with wavelength λ=1.5406A°, the current was 30mA and the voltage was 40 kv. The scanning angle 2θ was varied in the range of 20 – 60 degree with speed of 4 deg/min. The inter planer distance d_{hkl} for different planes was determined by using Bragg's law[56]:

$$n\lambda = 2d\sin\theta \quad \ldots\ldots\ldots\ldots\ldots\ldots(3\text{-}3)$$

Where n is the reflection order and θ is Bragg's angle.

(3-9) The Electrical Measurements

D.C. conductivity and Hall effect for Cd_XSe_{1-X} films deposited on glass substrate at room temperature with (Al) electrodes were measured.

3-9-1 D.C. Conductivity Measurement

The electrical conductivity has been measured as a function of temperature for Cd_XSe_{1-X} films over the range (300 –478)K by using the electrical circuit. The measurements have been done using sensitive digital electrometer type keithley (616) and electrical oven as shown in fig (3.8)

The resistivity (ρ) of the films is calculated by using the following equation:

$$\rho = \frac{R.A}{L} \quad \ldots\ldots\ldots\ldots\ldots\ldots(3\text{-}4)$$

where R is the sample resistance, A is the cross section area of the films and L is the distance between the electrodes. The conductivity of the films was determined from the relation:

$$\sigma_{d.c} = \frac{1}{\rho} \ldots\ldots\ldots\ldots\ldots\ldots(3\text{-}5)$$

The activation energies could be calculated from the plot of lnσ versus 1000/T according to equation (2-5).

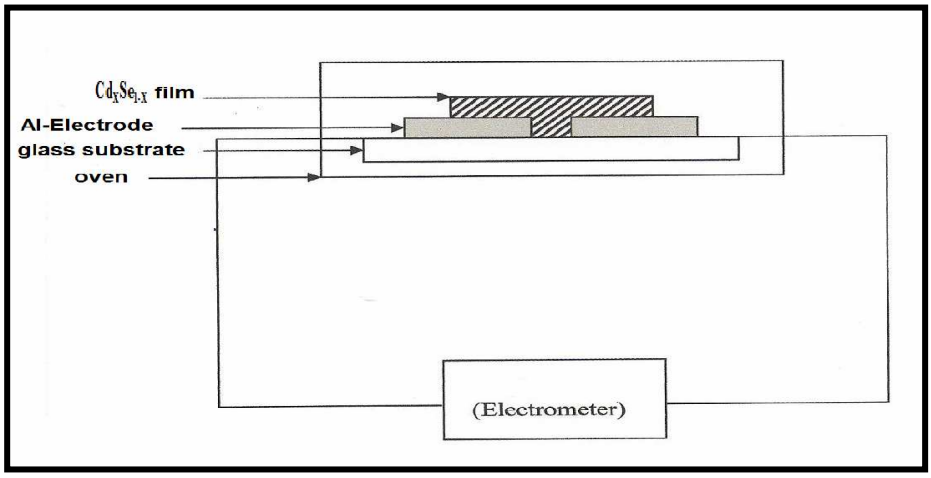

Figure (3.8) The circuit used for measuring D.C. conductivity

3-9-2 A.C.Conductivity

The Cd_XSe_{1-X} samples were prepared in sandwich configuration between (Al) foils (400nm thickness and the diameter=0.5cm) thin film electrodes, the samples and (Al) electrode are deposited on to glass substrate using mask as shown in fig.(3-3b). For ac- measurement, an HP-R2C unit model (4275 A) multi frequency LCR meter has been used to measure the capacitance (C) and resistance (R) with frequency range between 100Hz-100kHz,with an accuracy of 0.1%, as shown in fig(3.9) . Ac instrument is shielded by the copper sheet to avoid the distortion signal, and to prohibit the connectors among the experimental portion from becoming a source of noise by using coaxial cables and BNC connectors were used.

The amplitude of measuring ac signal was kept low at 0.08 volt to avoid possible non linearity and instability.

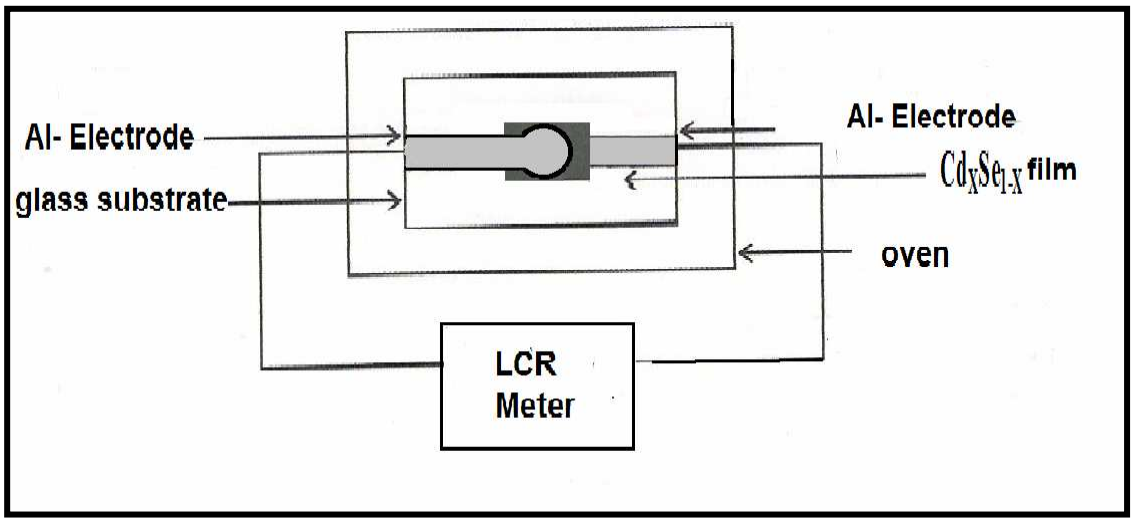

Figure (3.9) The circuit used for measuring A.C. conductivity

3-9-3 Hall Effect Measurements

The Hall effect measurement was carried out according to the electrical circuit shown in Fig. (3.10), which contains D.C. power supply with 0 – 40 volt and two digital electrometers (Keithley type 616) to measure the current and voltage. When the magnetic field (B = 0.257 Tesla) is applied perpendicular to the applied electrical field, a transverse e.m.f. which is called Hall voltage (V_H) is set up across the sample. So that the Hall coefficient is given by[56].

$$R_H = \frac{V_H}{I} \cdot \frac{t}{B} \quad \text{..... (3-6)}$$

The sign of Hall coefficient determines the type of charge carrier. The carrier concentration (n_H) is related to the Hall coefficient which is given by:

$$R_H = \frac{-1}{n \cdot q} \quad \text{.....(3-7)} \qquad \text{for n-type}$$

$$R_H = \frac{1}{p \cdot q} \quad \text{..... (3-8)} \qquad \text{for p-type}$$

Hall mobility (μ_H) could be calculated simply from the product of the conductivity σ and the Hall coefficient according to equation:

$$\mu_H = \sigma |R_H| \text{.....(3-9)}$$

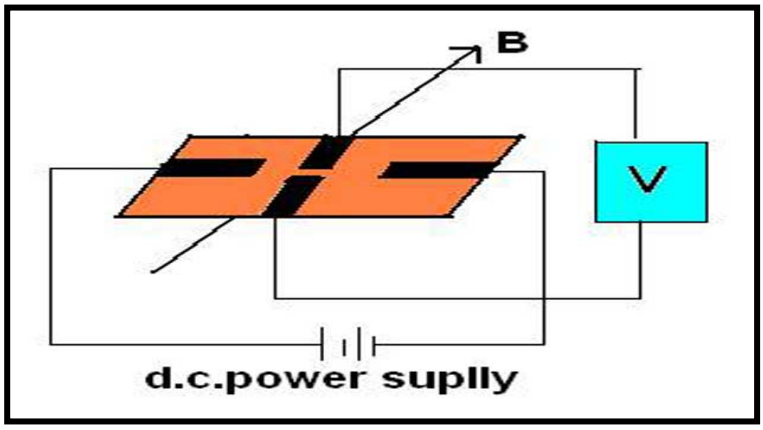

Figure (3.10): The circuit diagram for Hall measurement

Chapter Four

Results and Discussion

(4-1) Introduction:

This chapter includes the results and the analysis of the experimental measurements, which involve the structural and electrical properties of Cd_XSe_{1-X} films which prepared by thermal evaporation at different concentration (X=0.1,0.2,0.3,0.4) at (t=400 nm, T_s=300 K), different thicknesses (t=200,300,400,500)nm at (X=0.3 and T_s=300 K) ,and different substrate temperatures (300,348,373,393) K at (X=0.3 and t=400 nm) .

(4-2) Structural Properties :

The X-ray diffraction (XRD) patterns for (Cd_XSe_{1-X}) powders, which prepared experimentally at different concentration (X=0.1 ,0.2 ,0.3 ,and 0.4), are shown figures (4.1),(4.2),(4.3),and (4.4) respectively.

The observation of X-ray peaks in all (Cd_XSe_{1-X}) powders indicates that the structure of these alloys are polycrystalline .Table (4.1) lists the observed the d-values with standard (JCPDS-ICDD file NO, 8-0459,and 19-0191) for CdSe compound .The observed of the d-values for Cd_XSe_{1-X} powder at (X=0.1,0.3,and 0.4) are in agreement with the standard values for the hexagonal and cubic structure ,while the d-values for Cd_XSe_{1-X} powder at (X=0.2) are agreement with standard values for hexagonal structure . (Goldschmidt,1960)[57] pointed that the direct combination of the elements gives a hexagonal of wurtzite type for the CdSe compound.

Table (4.1): X-ray diffraction data for Cd $_X$Se$_{1-X}$ powders .

X	2θ (deg)	d (A^0)	hkl
0.1	24.08	3.692	100
	25.348	3.51	111
	26.98	3.302	101
	35.109	2.55	102
	36.618	2.45	033 (Se) mono
	41.4	2.17	110
	44.116	2.05	134 (Se) mono
	48.651	1.87	200
	49.673	1.8339	112
	55.603	1.65	202
0.2	23.887	3.72	100
	27.109	3.28	101
	35.112	2.55	102
	41.4	2.179	110
	43.96	2.058	134 (Se) mono
	45.63	1.986	103
	49.66	1.834	112
0.3	23.849	3.278	100
	25.35	3.51	111
	27.076	3.29	101
	35.122	2.553	102
	41.97	2.151	110
	43.99	2.056	134 (Se) mono
	45.78	1.98	103
	49.67	1.8343	112
0.4	23.774	3.73	100
	25.26	3.52	111
	27.12	3.28	101
	35.114	2.55	102
	42.081	2.145	110
	45.67	1.984	103
	49.668	1.83409	112

From figure (4.1,2,3), it is quite apparent the X-ray diffraction of powder, with (X=0.1,0.2,0.3) , shows many peaks related to the planes (134) and (033), which related to selenium (Se) ,due to the high concentration of selenium (Se).

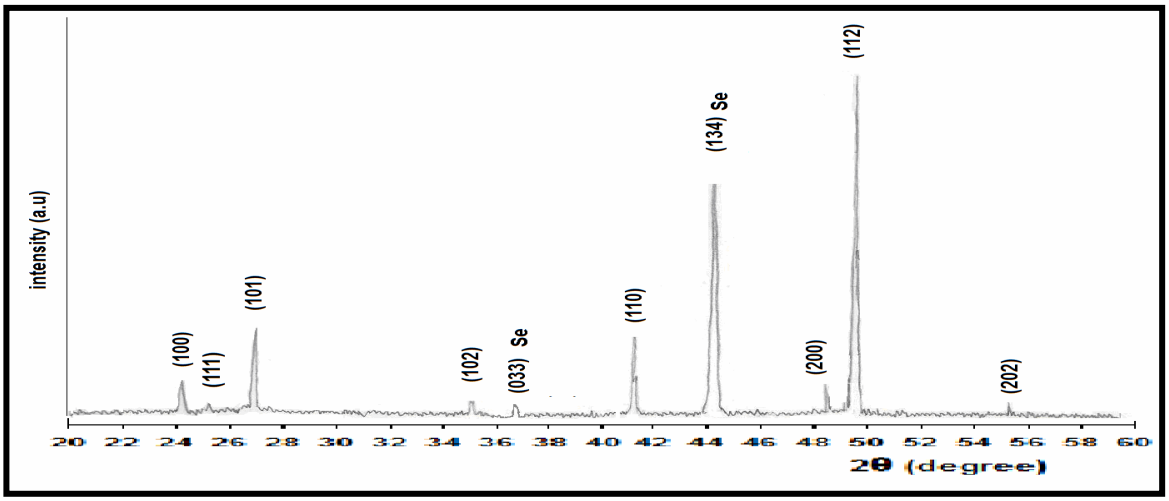

Figure (4.1):X-ray diffraction pattern of $Cd_X Se_{1-X}$ powder with X=0.1

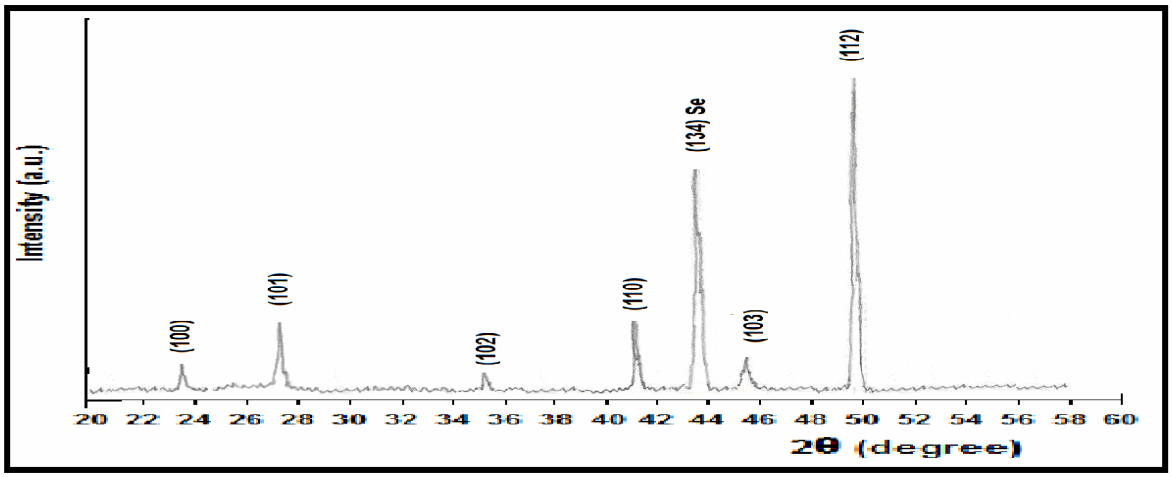

figure (4.2): X-ray diffraction pattern of $Cd_X Se_{1-X}$ powder with X=0.2

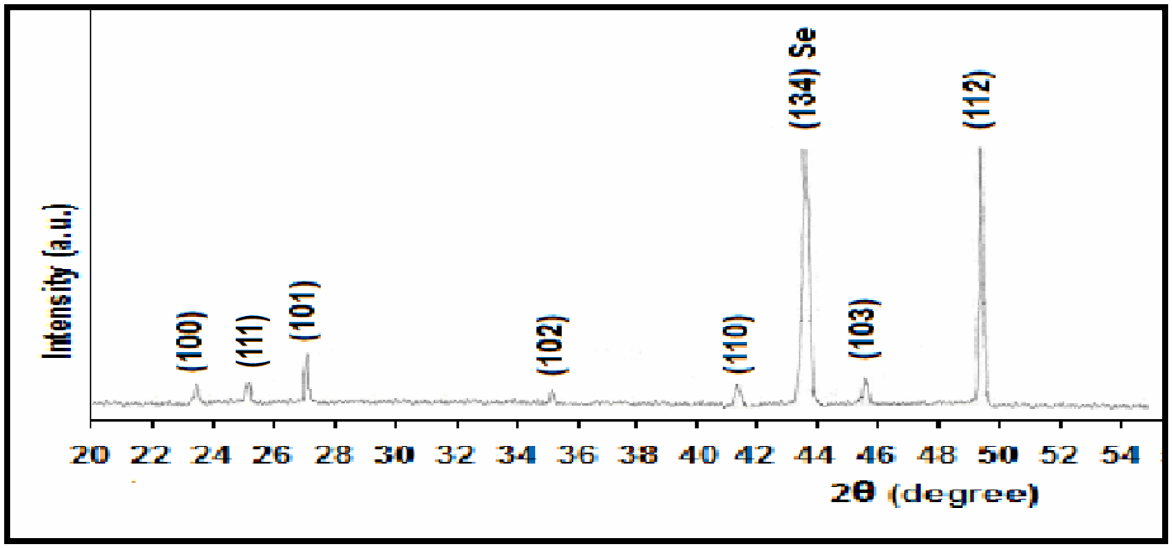

figure (4.3): X-ray diffraction pattern of $Cd_X Se_{1-X}$ powder with X=0.3

and from figure (4.4) it is apparent that the X-ray diffraction of $Cd_X Se_{1-X}$ powder with (X=0.4) there is no peaks related to selenium.

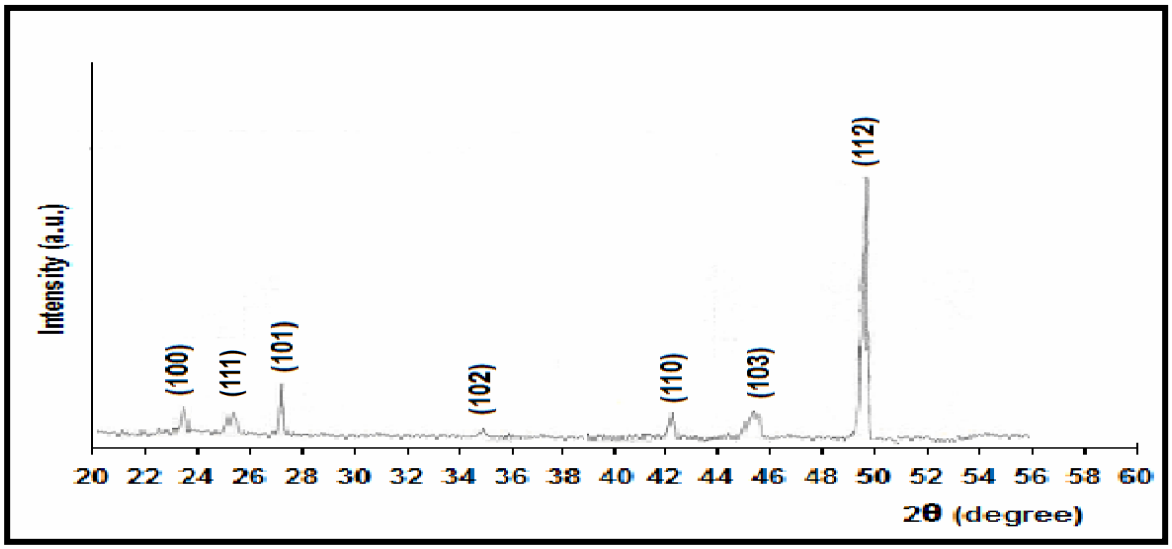

figure (4.4): X-ray diffraction pattern of Cd_XSe_{1-X} powder with X=0.4

By studying the crystal structure of Cd_XSe_{1-X} films, which prepared from ($Cd_X Se_{1-X}$) powder with a prior mentioned concentrations as listed in table (4.2) .All the films are polycrystalline structure and mixture of cubic and hexagonal unit cell at (X=0.1,0.3, 0.4),but only cubic unit cell at (X=0.2) . with peaks of plane (031),(134) for selenium (Se),due to the high concentration of (Se) in a film at (X=0.1) as shown in figure(4.5) , and (100) at (X=0.2) as shown in figure (4.6). The preferred orientation lies along [111] direction .

Table (4.2): X-ray diffraction data for Cd_XSe_{1-X} films.

X	t(nm)	T_S(K)	2θ (deg)	d (A^0)	hkl
0.1	400	300	23.89	3.72	100
			25.325	3.5139	111
			27.08	3.29	101
			29.743	3.001	031 (Se) mono
			35.137	2.55	102
			41.94	2.15	110
			44.48	2.035	134 (Se) mono
			49.708	1.834	112
0.2	400	300	23.454	3.7899	100 (Se)
			25.417	3.501	111
0.3	200	300	25.414	3.5018	111
			26.794	3.324	101
			45.698	1.984	103
			50.781	1.797	201
	300	300	25.386	3.505	111
			26.781	3.326	101
			45.589	1.943	103
			50.734	1.798	201
	400	300	25.414	3.501	111
			26.827	3.3024	101
			45.49	1.992	103
			50.5	1.805	201
		348	23.479	3.78	100 (Se)
			25.4577	3.496	111
			45.5804	1.988	103
		373	23.526	3.77	100 (Se)
			25.457	3.496	111
			29.772	2.998	101 (Se)
			45.887	1.976	103
		393	23.392	3.799	100 (Se)
			25.471	3.494	111
			29.702	3.005	101 (Se)
			45.786	1.98	103
	500	300	25.459	3.494	111
			26.866	3.315	101
			45.753	1.981	103
			50.746	1.797	201
0.4			25.457	3.496	111
			45.73	1.98	103

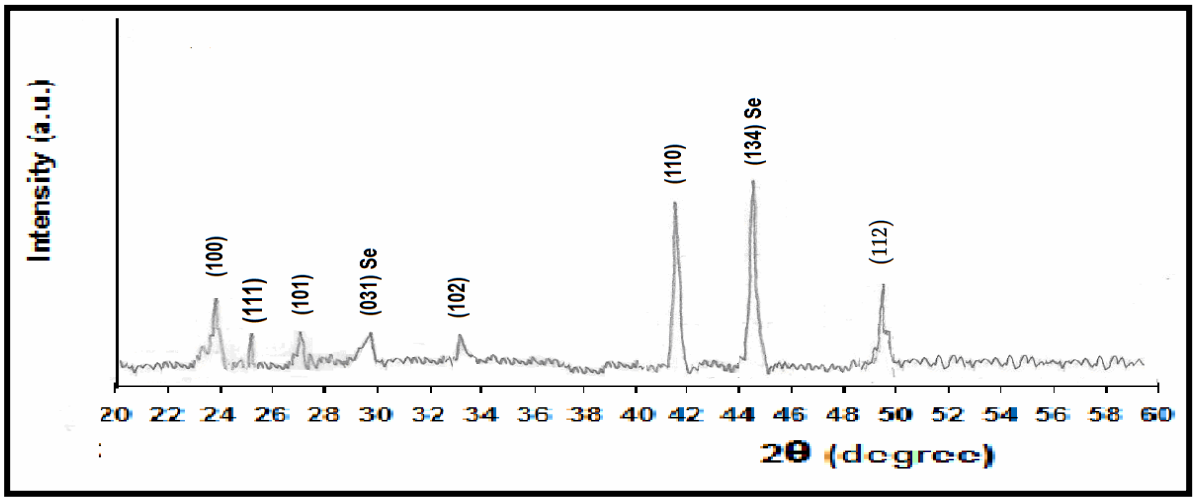

figure (4.5): X-ray diffraction pattern of Cd_XSe_{1-X} film with X=0.1

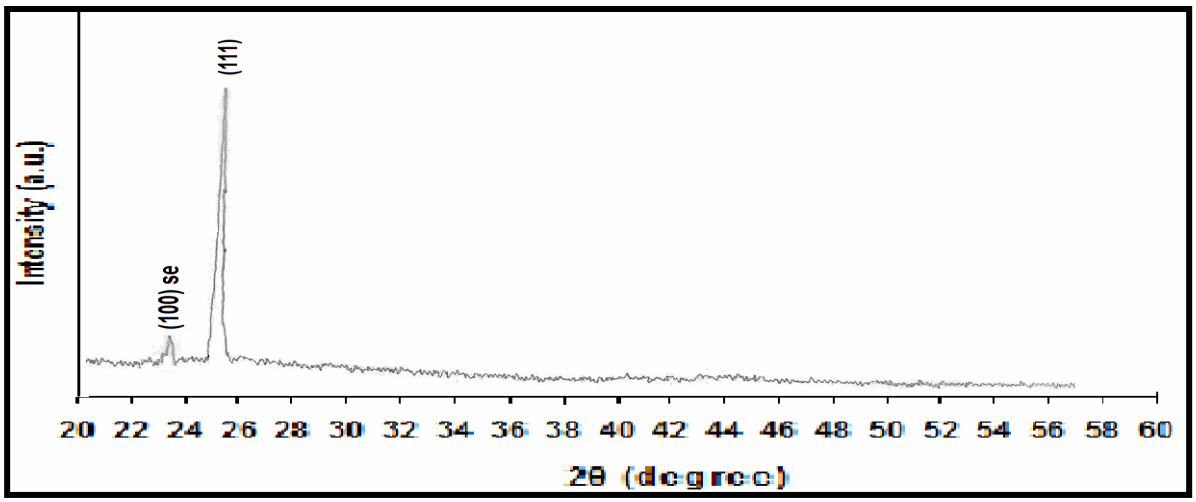

figure (4.6): X-ray diffraction pattern of Cd_XSe_{1-X} film with X=0.2

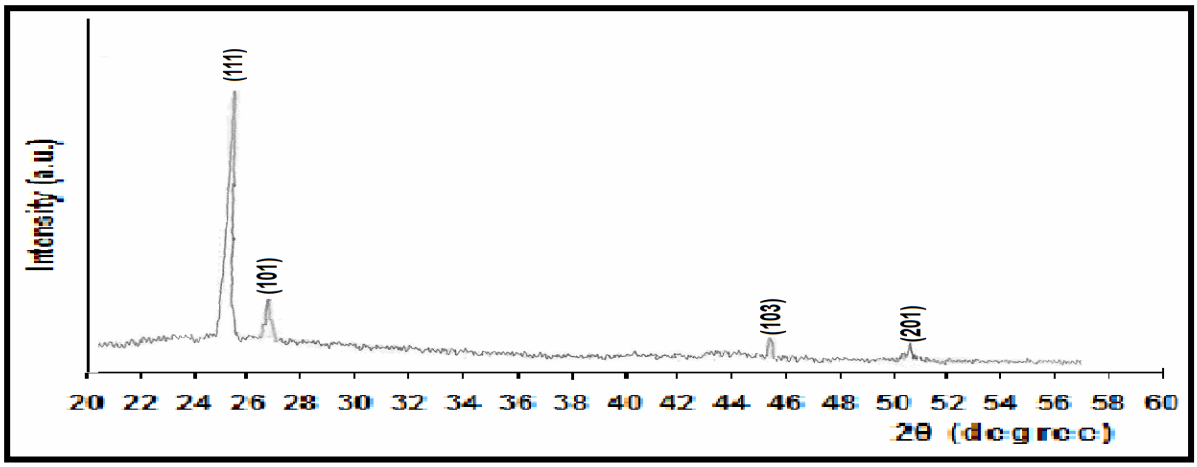

figure (4.7): X-ray diffraction pattern of Cd_XSe_{1-X} film with X=0.3

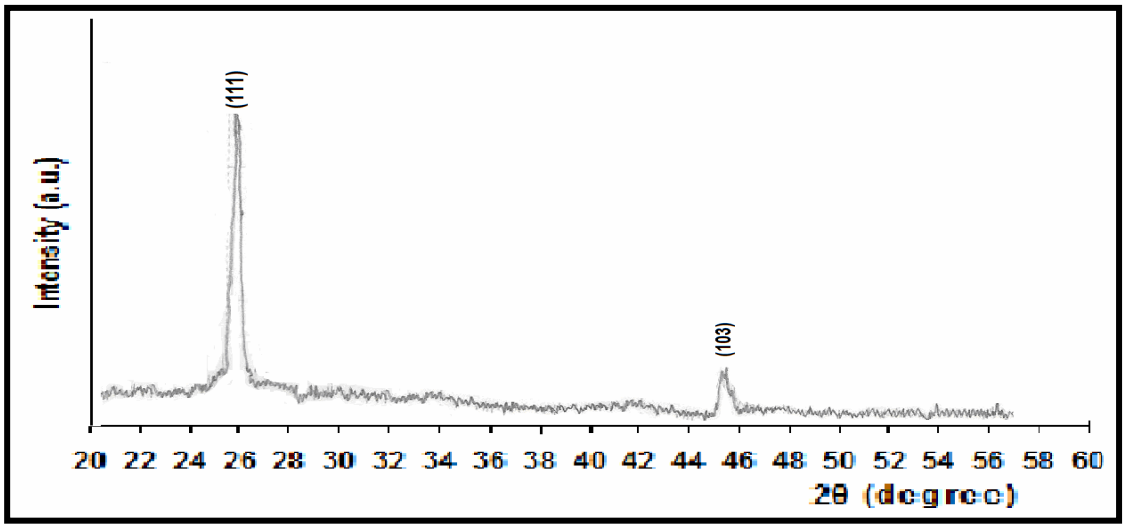

figure (4.8): X-ray diffraction pattern of Cd_XSe_{1-X} film with X=0.4

The XRD patterns for Cd_XSe_{1-X} films at (X=0.3) and (T_s=300 k) with different thicknesses (200,300,400,500 nm); indicate that the samples are polycrystalline and have a mixture of wurtzite (hexagonal) and cubic structure. The crystallites are preferentially oriented with the (111) plane ,as shown in figures(4.7),(4.9),(4.10),(4.11),and Table (4.2).

The XRD patterns for Cd_XSe_{1-X} films at (X=0.3) and (t=400 nm) with different substrate temperatures (300,384,373,393 K), indicate that the samples are polycrystalline structure and mixture of cubic and hexagonal unit cell, this results are agreement with (Izzat M.Al-Essa 2008)[58],as shown in figures(4.7),(4.12),(4.13),(4.14) ,and Table (4.2).The effect of increasing the substrate temperatures was clear in the crystalline structure of the films by appearance new peak relate to (100) and (101) planes for selenium (Se) with hexagonal phase.

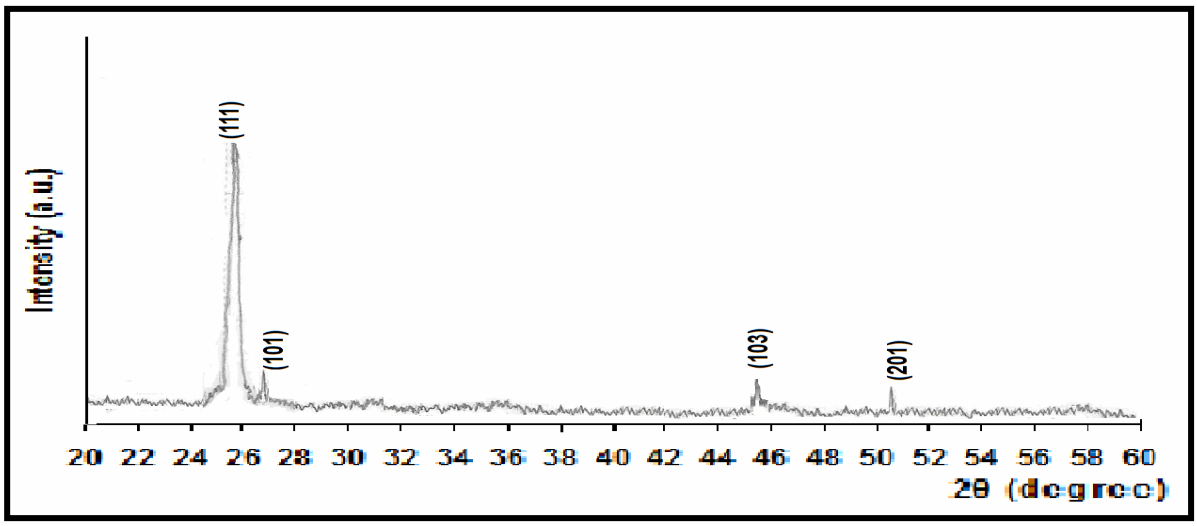

figure (4.9): X-ray diffraction pattern of $Cd_{0.3}Se_{0.7}$ film with t=200 nm

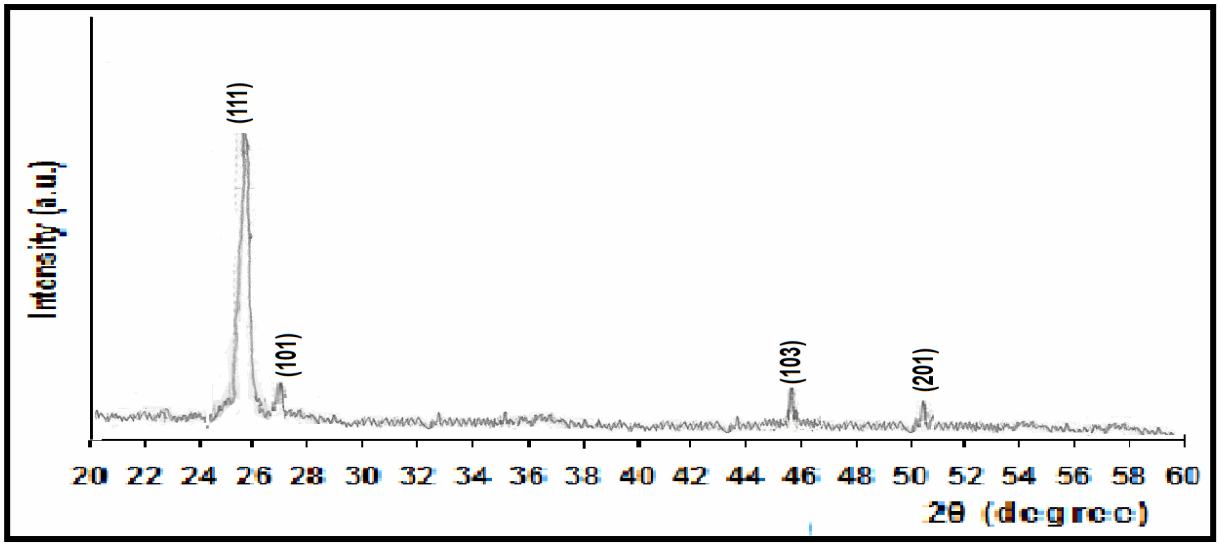

figure (4.10): X-ray diffraction pattern of $Cd_{0.3}$ $Se_{0.7}$ film with t=300 nm

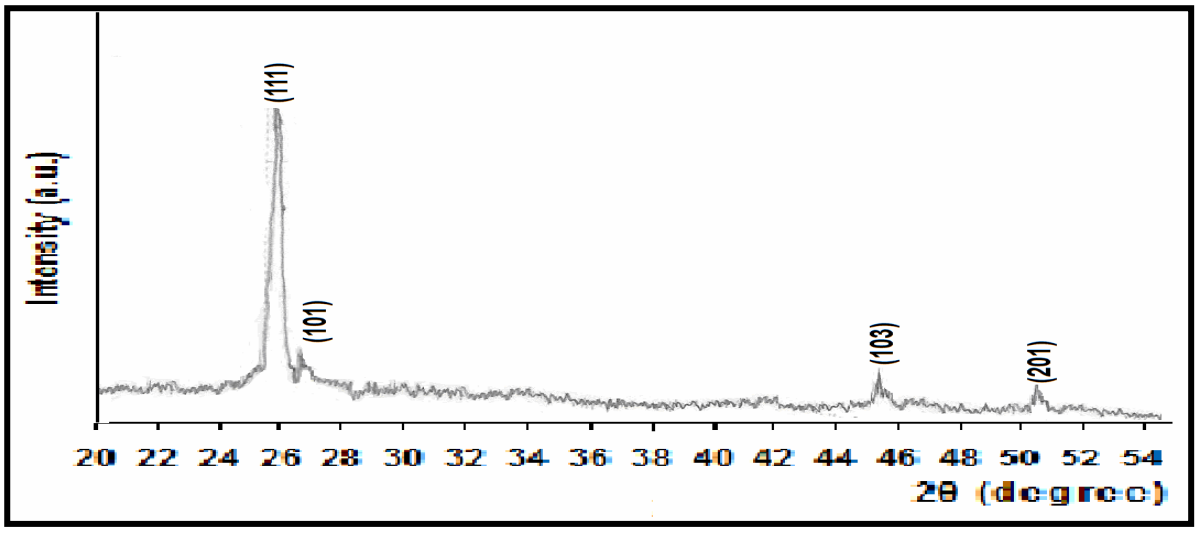

iguref (4.11): X-ray diffraction pattern of $Cd_{0.3}$ $Se_{0.7}$ film with t=500 nm

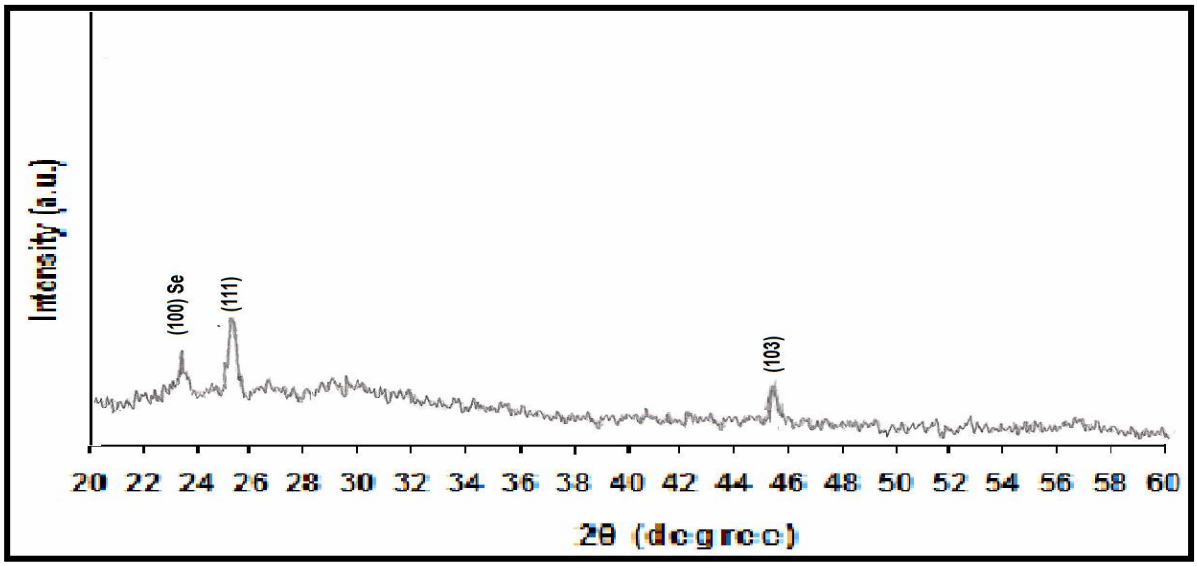

Figure (4.12): X-ray diffraction pattern of $Cd_{0.3}Se_{0.7}$ film with T_s= 348 K, and t=400nm

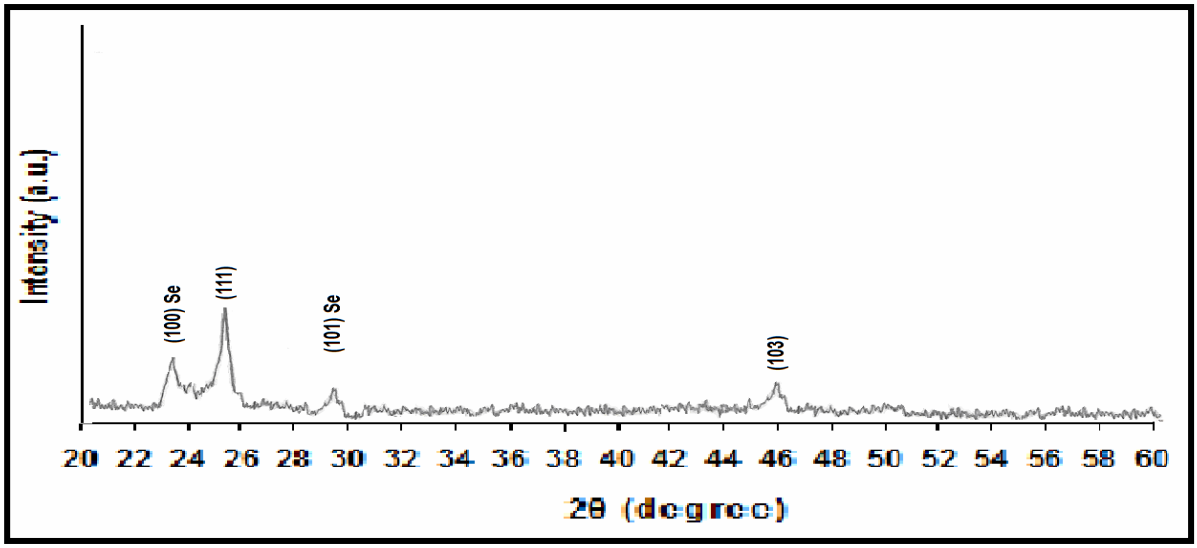

Figure (4.13): X-ray diffraction pattern of $Cd_{0.3}Se_{0.7}$ film with T_s= 373 K, and t=400nm

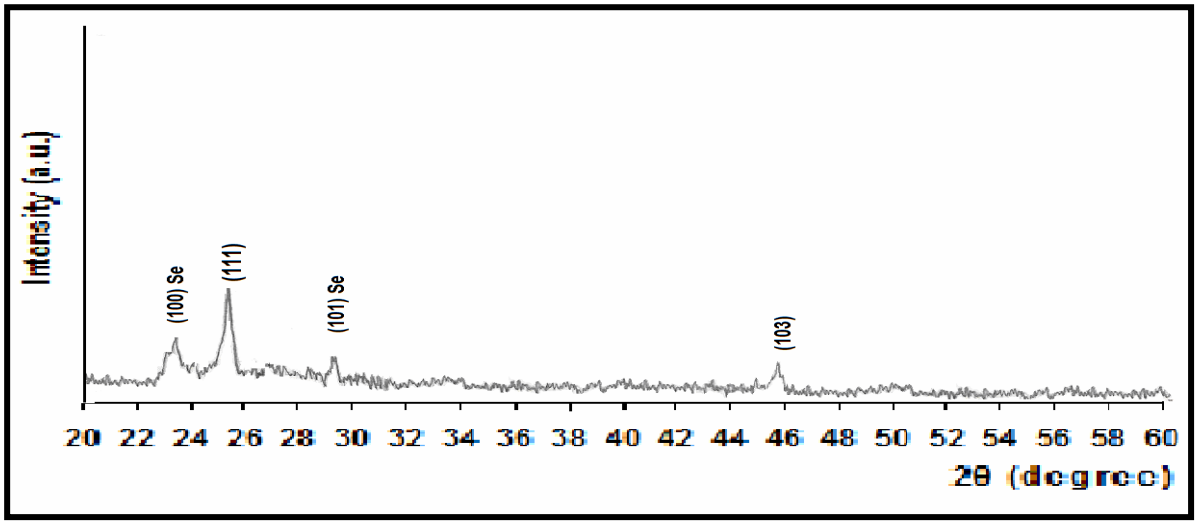

Figure (4.14) :X-ray diffraction pattern of $Cd_{0.3}$ $Se_{0.7}$ film with T_s= 393 K and t=400nm

(4-3) D.C Conductivity:

The (d.c) conductivity ($\sigma_{d.c}$) for Cd_XSe_{1-X} films has been studied as a function of (T) with the range of (300-473 K), at different value of (X=0.1, 0.2, 0.3, 0.4) with thickness (t=400 nm) and substrate temperature (T_s=300 K).

The ($\sigma_{d.c}$) of Cd_XSe_{1-X} films decreases as the Cd concentration (X) decreases (i.e decreases as increases the (Se) concentration), this is due to the higher resistivity of (Se).from figures(4.15,a,b,c,d) ; it is found there are two stages of conductivity throughout the heating temperature range.

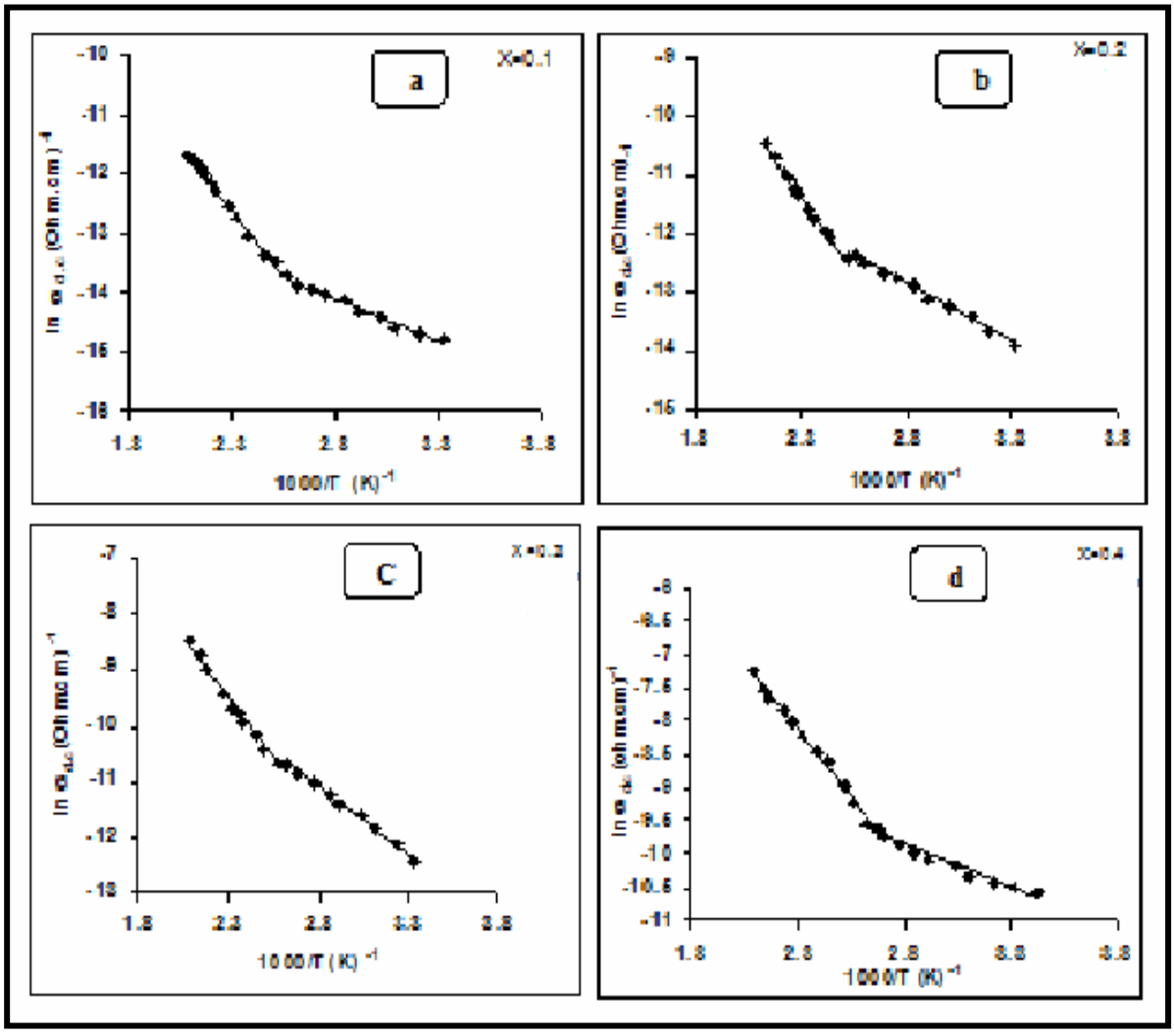

Figure (4.15): ln σ versus 1000/T for Cd_XSe_{1-X} films at different concentration (X) (a): 0.1 (b): 0.2 (c): 0.3 (d): 0.4 and (t=400 nm, T_s=300 K).

The first activation energy (E_{a1}) occurs at low temperatures with the range (300-393 K)the conduction mechanism of this stage is due to carriers transport to localized states near the valence band. While the second activation energy (E_{a2}) occurs at high temperatures with in the range (393-437 K) ,and it is due to conduction of the carrier excited into the extended states beyond the mobility edge. As listed in Table (4.3); the activation energy and conductivity takes unstable behavior with increasing the concentration (X) , due to the change in the phase of structure.

From figures(4.16,a,b,c,d) it is found that the ($\sigma_{d.c}$) conductivity of Cd_XSe_{1-X} films at (X=0.3) with different substrate temperatures (300-393 K), and thickness (t=400 nm) that the conductivity decreases with increasing the substrate temperatures (T_s), this is because of the high concentration of (Se) in the films. The value of activation energies are listed in Table (4.3) it was calculated that there are two activation energies E_{a1} and E_{a2} , which decreases with increasing the substrate temperature due to increases the energy gap, this is because the increasing of (Se) lead to increased energy gap, as is evident from the X-ray examinations, where appeared peaks of (Se) with increasing the substrate temperature..

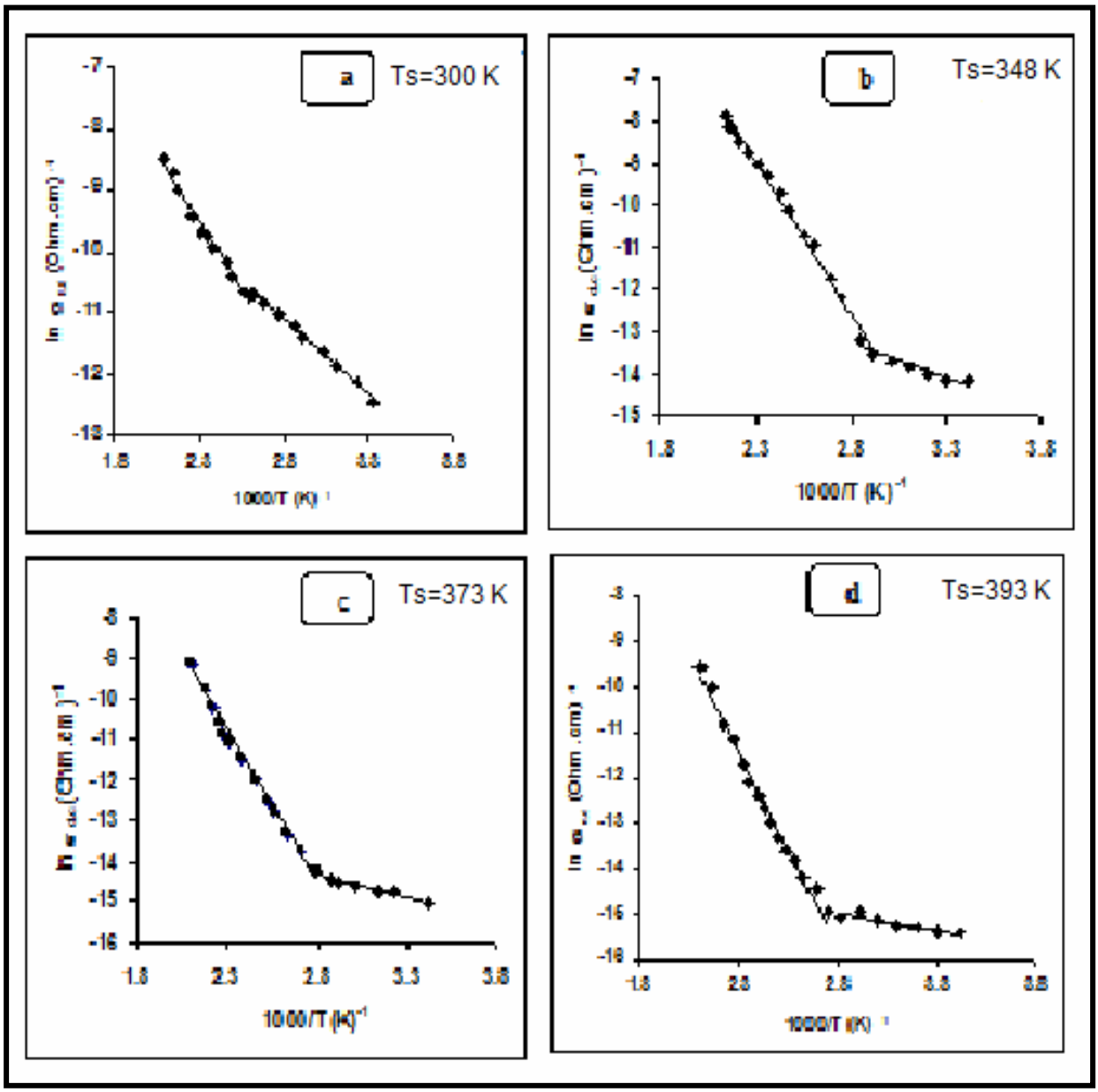

Figure (4.16): ln $\sigma_{d.c}$ versus 1000/T for $Cd_X Se_{1-X}$ films at different substrate temperatures (a): 300 K (b): 348 K(c): 373 K (d): 393 K and (t=400nm ,X=0.3).

From figures(4.17,a,b,c,d) and table (4.3) it can be see that the value of electrical conductivity tends to increase with increasing in film thickness. The low electrical conductivity of thinner film is attributed to the existence of an island structure , which contain many defect sites ,so the defect density is much smaller for thicker films , as results the electrical conductivity of the films increases with film thickness[59] . The observed lesser conductivity in thinner films can be explained due to lower degree of crystalline. This result is in agreement with Padiyan *et al*.[60] Also it is clear that the activation energies increasing with increasing of thickness, may be due to decreases in absorption and increase in energy gap with increase of thickness.

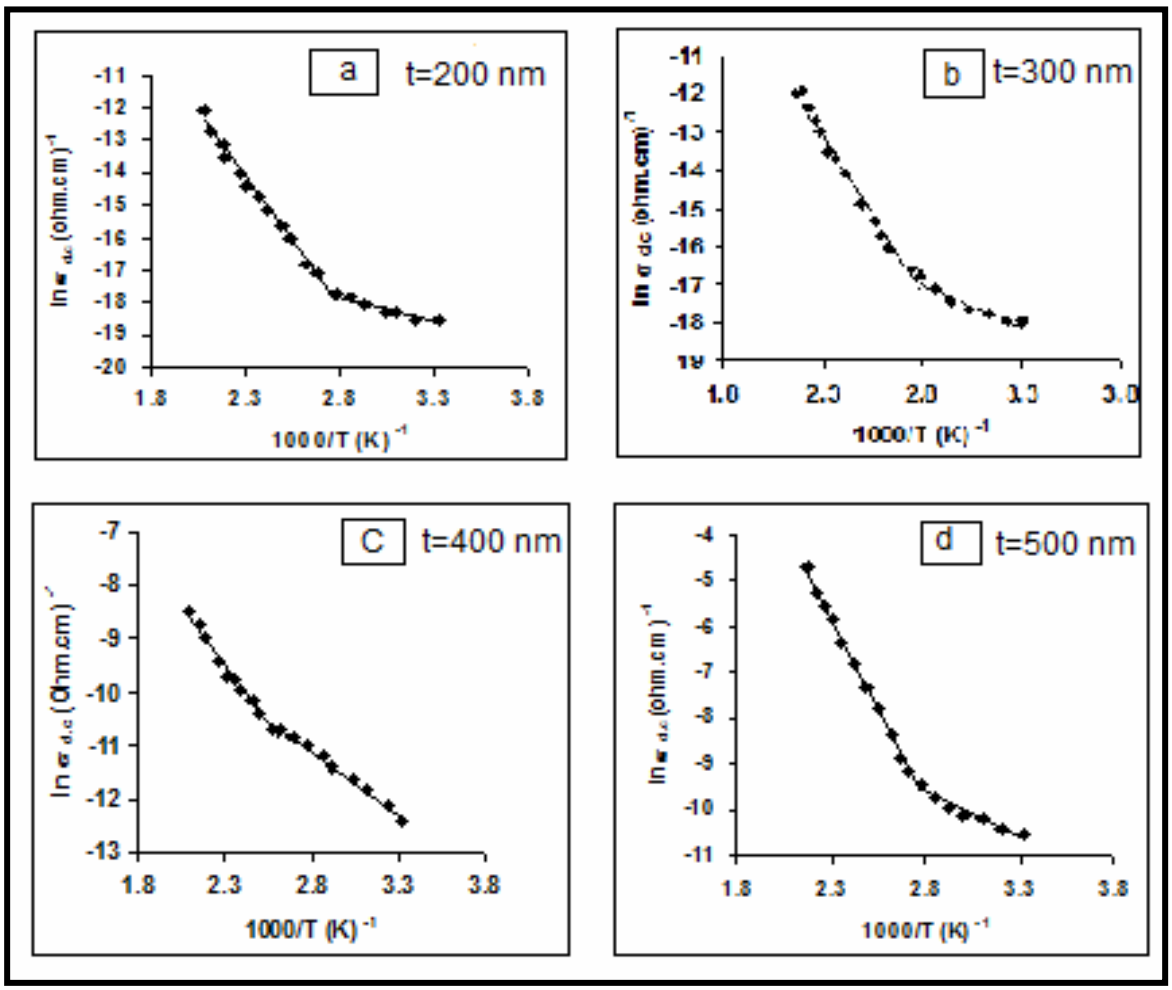

Figure (4.17): ln $\sigma_{d.c}$ versus 1000/T for Cd $_X$ Se $_{1-X}$ films at different thicknesses (a): 200 nm (b): 300 nm (c): 400 nm (d): 500 nm, and (X=0.3,T_s=300 K)

Table(4.3): D.C. conductivity parameters for Cd_XSe_{1-X} films at different concentration, thicknesses and substrate temperatures.

Concentration (X)	Thickness (t) nm	T_s (K)	E_{a1} (eV) Range (K)	E_{a2} (eV) Range (K)	$\sigma_{R.T} \times 10^{-6}$ $(\Omega.cm)^{-1}$
0.1	400	300	0.124 300-393 K	0.633 393-473 K	6.13
0.2	400	300	0.156 300-393 K	0.649 393-473 K	0.68
0.3	200	300	0.213 300-357 K	0.801 367-473 K	0.009
	300	300	0.188 300-357 K	0.725 367-473 K	0.015
	400	300	0.133 300-393 K	0.215 393-473 K	2.76
		348	0.142 300-423 K	0.324 423-473 K	0.83
		373	0.166 300-423 K	0.437 423-473 K	0.304
		393	0.205 300-423 K	0.711 423-473 K	0.061
	500	300	0.094 300-357 K	0.327 367-473 K	27.4
0.4	400	300	0.085 300-393 K	0.551 393-473 K	45

(4-4)The Hall Effect:

The variation of Hall voltage as a function of currents for Cd_XSe_{1-X} films has been studied at different conditions when a magnetic field (B=0.257 Tesla) . These measurements show that the Cd_XSe_{1-X} films at (X=0.1, 0.2, 0.3, 0.4) are p-type as shown in figure(4.18,a,b,c,d), due to the presence of excess selenium which may produce cadmium vacancies in CdSe sites that form shallow acceptor level in the energy gap .From Table(4.4) we notice that the value of mobility decrease with increase (X),due to the high carrier concentration.

From figure(4.19,a,b,c,d) we found that all Cd_XSe_{1-X} films at (X=0.3) with different thicknesses and at (T_s=300 K) exhibit a positive Hall coefficient (p-type), and from Table (4.4) we observed that the carriers concentration decreases with increase of thickness.

The substrate temperature (T_S) considered as an effective parameter on the carrier concentration. From the figure(4.20,a,b,c,d) we found that all the films at (X=0.3) ,and (t=400 nm) exhibit a positive Hall coefficient(p-type) and from the Table (4.4) we notice that the carriers concentration decrease with substrate temperature increases may due to the re-crystallization process, which leads to the decrease of defects in the film during the film growth , and consequently a decrease of the carriers scattering at the defect, and the increasing of re-crystallization leads to rising the potential barrier, for that reason the mobility increasing.

Table (4.4) : Hall parameters for Cd_XSe_{1-X} films at different concentration , thickness and substrate temperature.

X	t (nm)	T_s (K)	n_H (cm^{-3})	μ_H(cm^2/v.s)
0.1	400	300	$3.84 * 10^{14}$	35.26
0.2	400	300	$6.71 * 10^{14}$	5.07
0.3	200	300	$11.16 * 10^{14}$	0.084
	300	300	$8.91 * 10^{14}$	0.391
	400	300	$8.66 * 10^{14}$	1.248
		348	$7.44 * 10^{14}$	1.85
		373	$4.6 * 10^{10}$	4.012
		393	$2.34 * 10^{10}$	6.371
	500	300	$8.33 * 10^{14}$	5.07
0.4	400	300	$2.1 * 10^{15}$	0.125

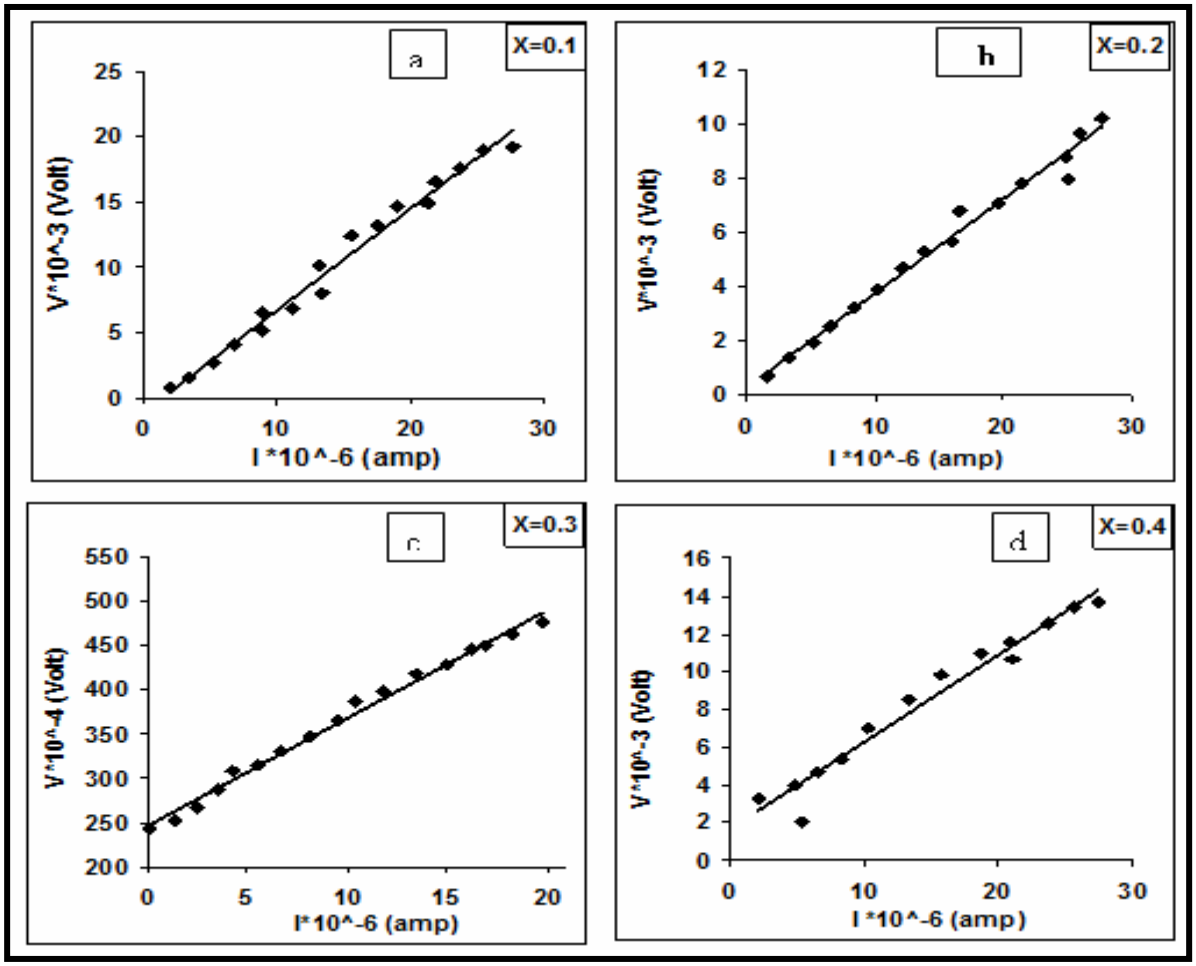

Figure (4.18): Variation of Hall voltage versus current for Cd_XSe_{1-X} films at different concentrations (a): 0.1 (b): 0.2 (c): 0.3 (d): 0.4 ,and (t=400 nm and T_s =300 k).

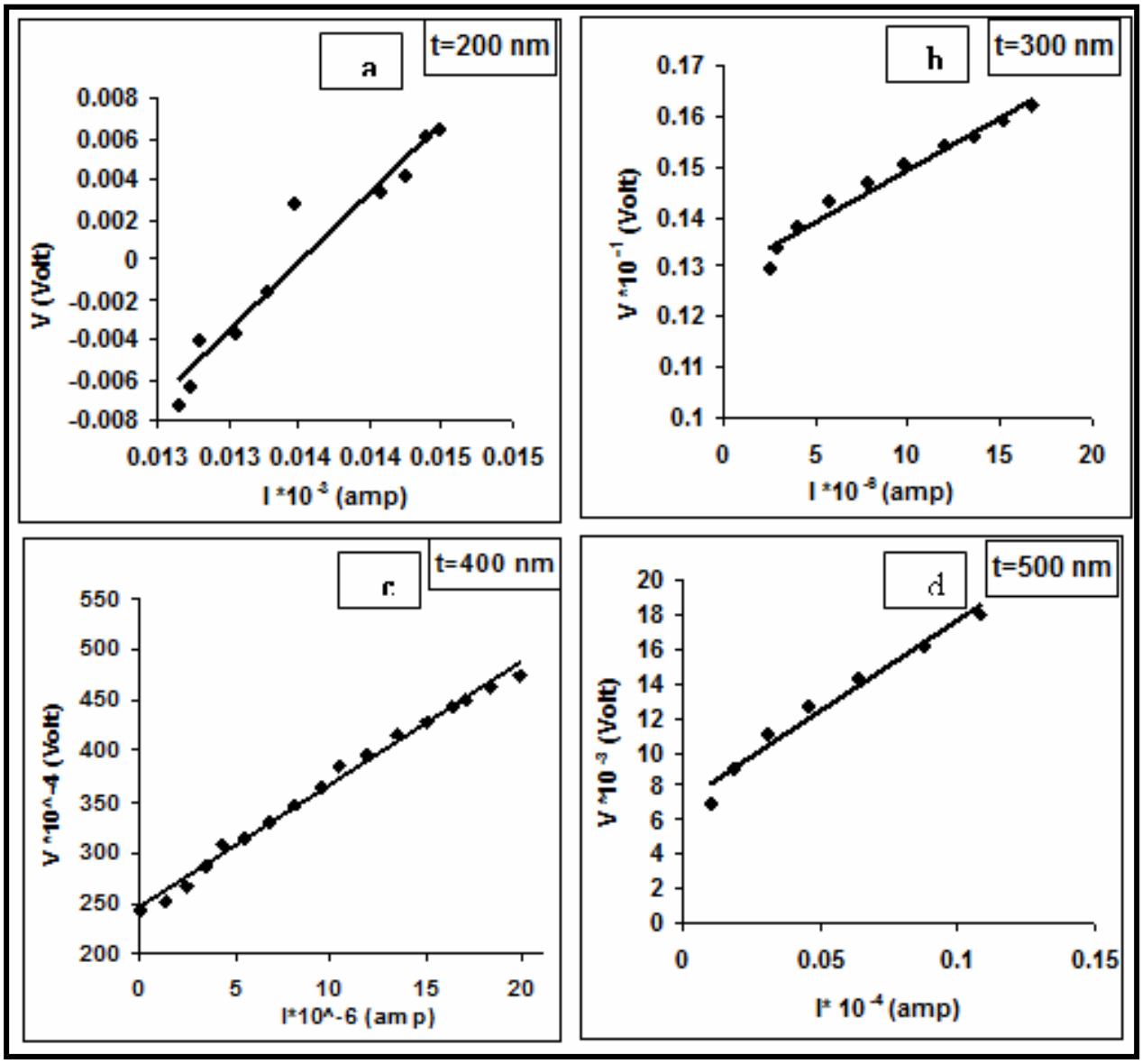

Figure (4.19): Variation of Hall voltage versus current for Cd_XSe_{1-X} films at different thickness (a): 200 nm (b): 300 nm (c): 400 nm (d): 500 nm ,and(X=0.3 , and T_s =300 K).

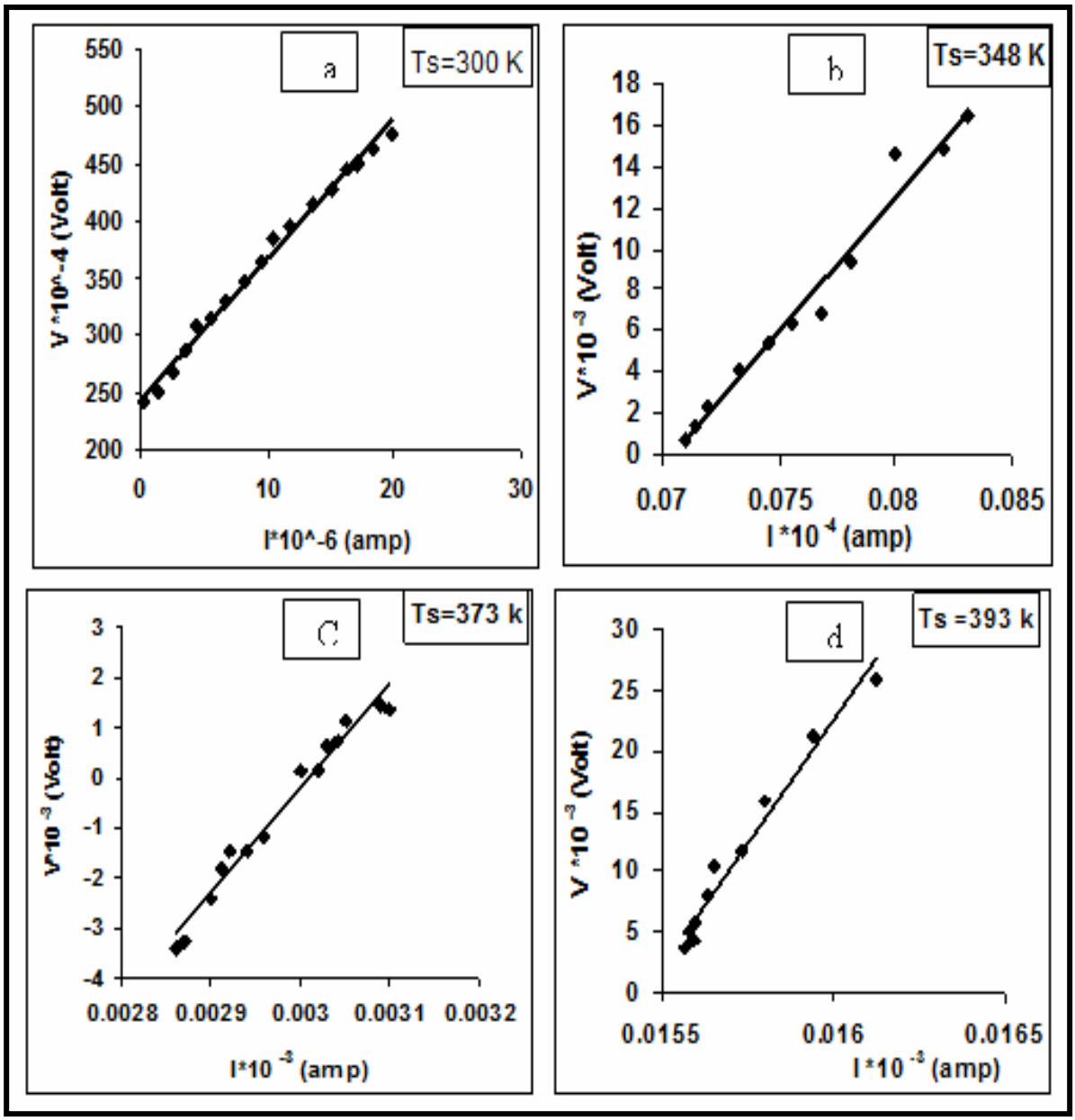

Figure (4.20): Variation of Hall voltage versus current for Cd_XSe_{1-X} films at different substrate temperature (a): 300 K (b): 348 K (c): 373 K (d): 393 K, and (X=0.3 and t=400 nm).

(4-5) A.C Conductivity:

The a.c conductivity measurement has been studied on the Cd_XSe_{1-X} thin films properties which prepared by different conduction such as concentration (X), thicknesses (t) , and substrate temperatures (T_s). From the frequency dependence of $\sigma(\omega)$ we can evaluate the exponent (s) and the temperature dependence of $\sigma(\omega)$ to calculate the activation energy $E(\omega)$, also the Cole-Cole diagram is drawn in order to find the polarizability (α) , dielectric constant (ε_s), and relaxation time (τ) for all the samples.

(4-5-1) Frequency Dependence on A.C conductivity:

All samples follow a common pattern where ln (σ_{tot}) is linear function of ln (ω). In other words $\sigma_{a.c}$ increases with increasing frequency according to equation (2-11) as shown in figure [4.21,22,23,(a,b,c,d)].In this case the $\sigma_{a.c}(\omega)$ dominates at higher frequency , in the range of ($10^3 - 10^5$)Hz. For lower frequency in the range of (10^2-10^3) Hz the conductivity becomes independent of the frequency because d.c conductivity dominate in this frequency range. The determination of a.c. conduction mechanism implies the study of the exponent (s) ; as a function of temperature. The dependence of exponent, s , on temperature is listed in table (4.5); it is observed that the smaller values of s have been observed for Cd_XSe_{1-X} at (X=0.3,t=400nm ,and T_S=300 K) and equal to (0.302), while the exponent S have a large value for Cd_XSe_{1-X} at (X=0.3,t=500 nm ,and T_S =300K) and equal to (0.91) . We observed the change in the exponent s is not systematic with the value of concentration (X), and substrate temperature (T_S) that is because of the change in the structure of there film ,as described in (4-2) paragraph .All films showed the same tend where ,s, decreases by increasing the annealing temperature .

This means that the correlated barrier hopping (C.B.H) model is the best model to explain the a.c. conductivity of Cd_XSe_{1-X} thin films

Table (4.5): Exponent (s) value of Cd_XSe_{1-X} films at different concentration thicknesses ,substrate temperatures and annealing temperatures.

Concentration X	t (nm)	T_s (K)	T_a (K)				
			300	313	333	353	373
			s	s	s	s	s
0.1	400	300	0.64	0.59	0.55	0.42	0.316
0.2	400	300	0.47	0.43	0.391	0.36	0.302
0.3	200	300	0.741	0.725	0.656	0.531	0.494
	300	300	0.82	0.781	0.707	0.7	0.61
	400	300	0.906	0.899	0.892	0.84	0.81
		348	0.554	0.529	0.496	0.442	0.399
		373	0.85	0.79	0.71	0.66	0.58
		393	0.66	0.59	0.505	0.492	0.471
	500	300	0.91	0.904	0.79	0.77	0.61
0.4	400	300	0.83	0.76	0.65	0.41	0.321

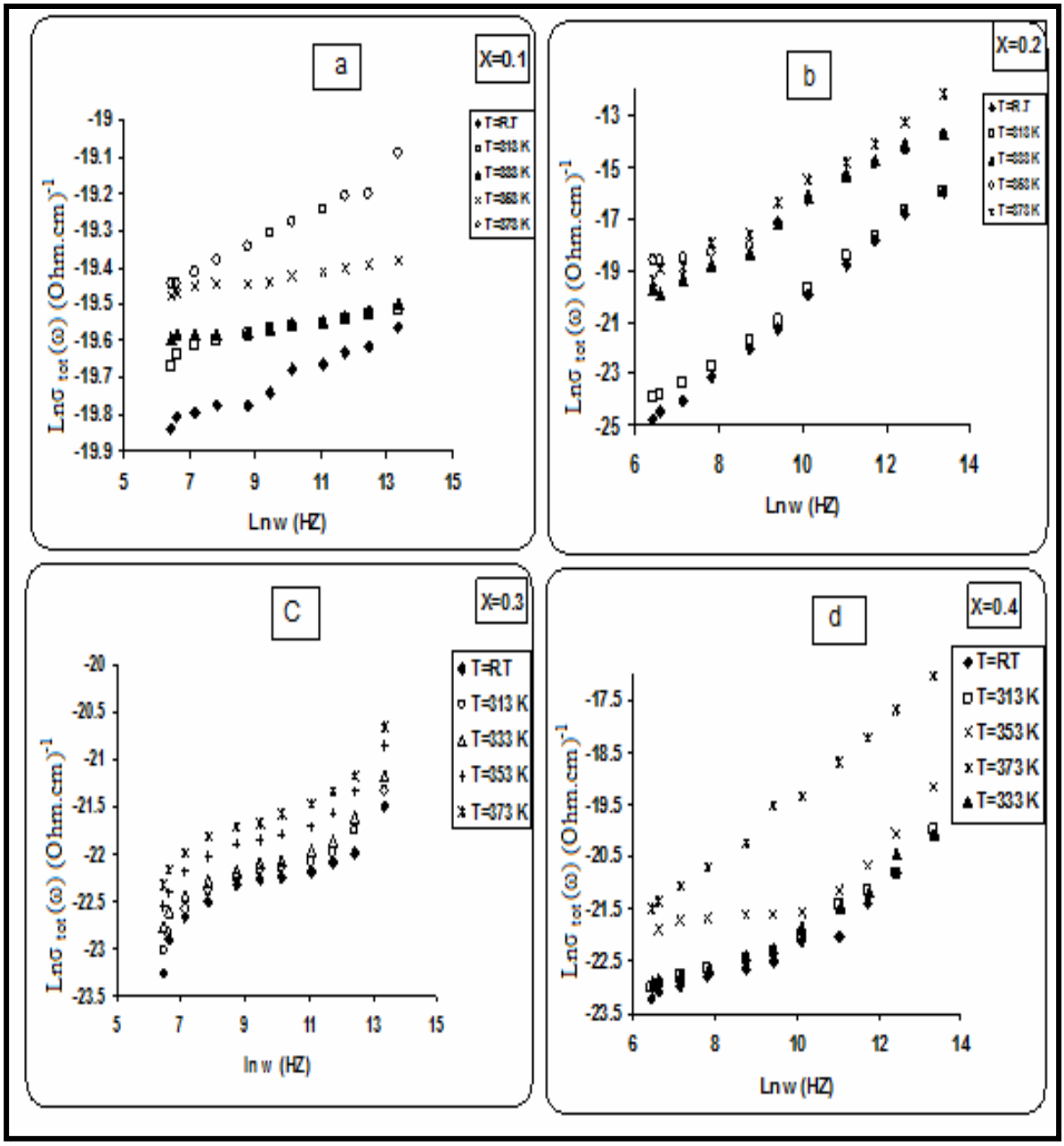

Figure(4.21,a,b,c,d) : ln σ_{tot} (ω) as a function of ln (ω) for Cd_XSe_{1-X} films at different concentration and annealing temperature (a): 0.1 (b): 0.2 (c): 0.3 (d): 0.4 and (t=400 nm, T_s=300 K).

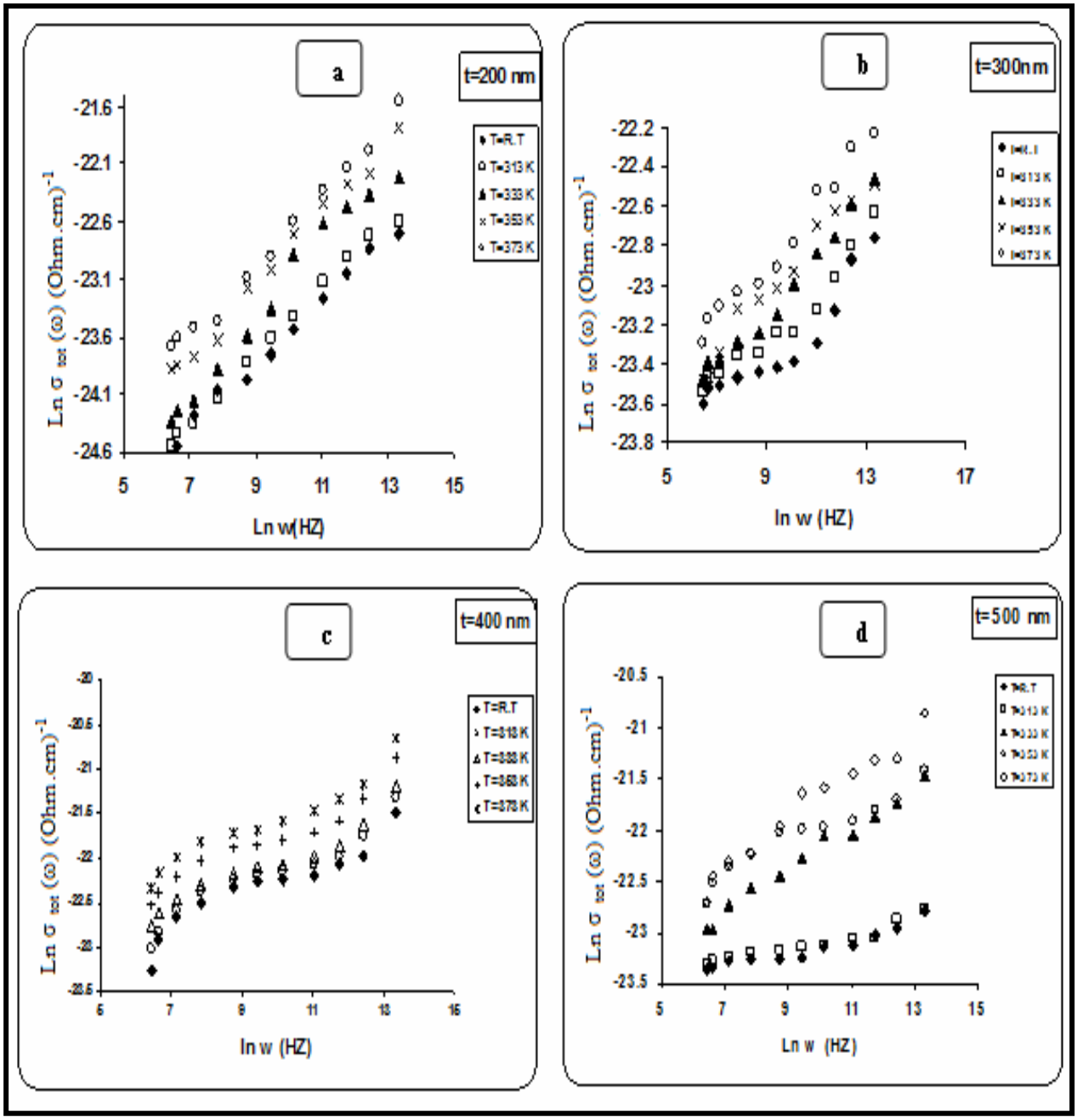

Figure(4.22,a,b,c,d) : : ln σ_{tot} (ω) as a function of ln (ω) for Cd_XSe_{1-X} films at different thickness and annealing temperatures(a): 200 nm (b): 300 nm (c): 400 nm (d): 500 nm, and (X=0.3,T_s=300 K)

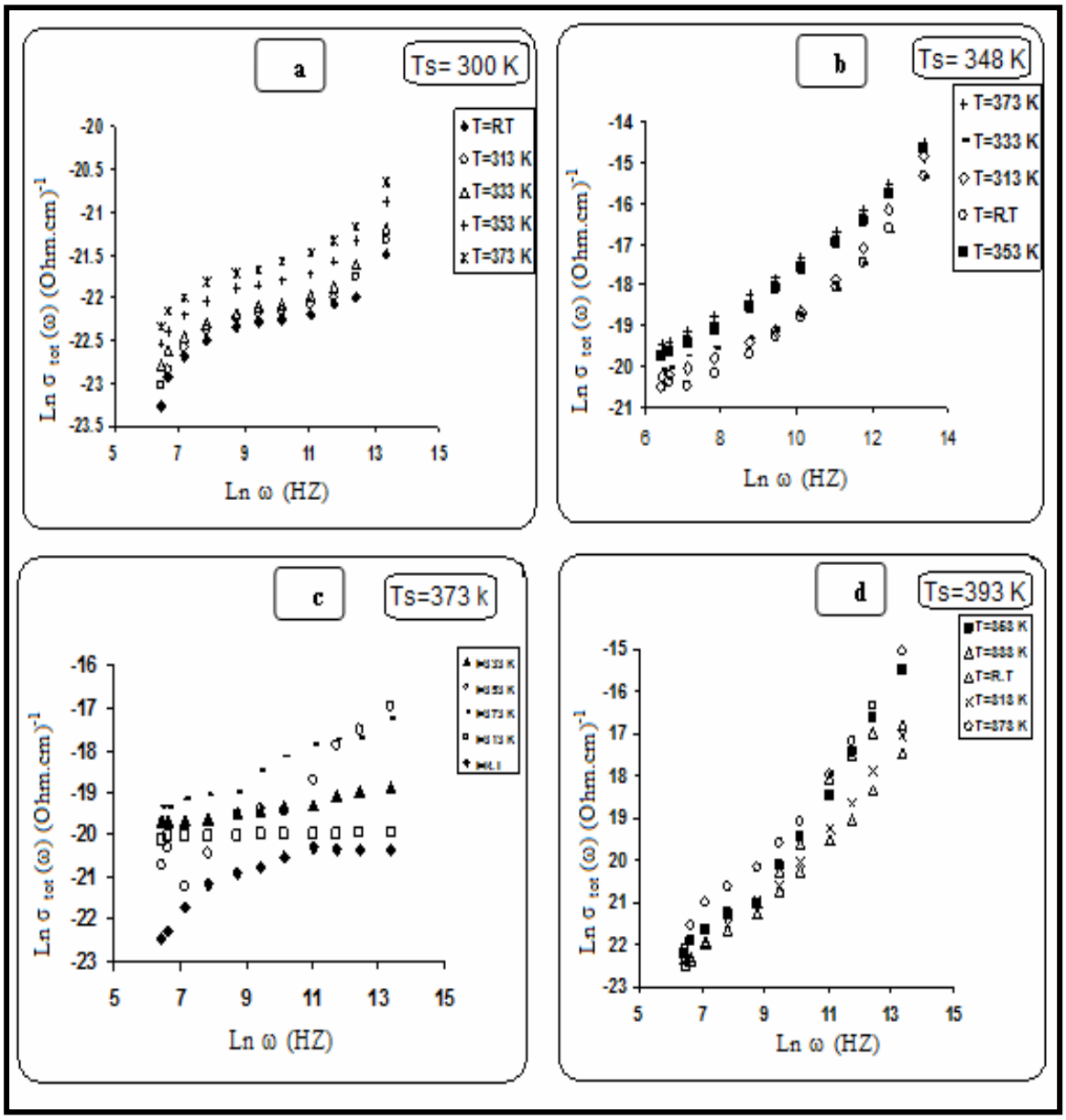

Figure(4.23,a,b,c,d) : : ln $\sigma_{tot}(\omega)$ as a function of ln (ω) for Cd_XSe_{1-X} films at different substrate temperatures and annealing temperatures (a): 300 K (b): 348 K(c): 373 K (d): 393 K and (t=400nm ,X=0.3).

(4-5-2)Temperature Dependence of A.C conductivity:

The variation of ln $\sigma_{a.c}(\omega)$ with reciprocal temperature ($10^3/T$) for Cd_XSe_{1-X} films for four fixed frequencies (10^2,10^3,10^4,10^5)Hz at different concentration (X),thicknesses, and substrate temperatures are shown in figures [4.24,25,26,(a,b,c,d)]. A linear behavior of $\sigma_{a.c}(\omega)$ of one stage has been observed over the entire temperature range indicating a thermal activated conduction mechanism. There is activation energy for each film less than the activation energy in the d.c conductivity because the dependence of a.c conductivity on the temperature being less than in the d.c conductivity. As shown in Table (4.6) the a.c activation energy E_ω is not systematic with the increasing of concentration because the change in a phase of structure as described in the (4-2) paragraph ; while the a.c activation energy decreases as the film thickness increases and this may be attributed to increase of absorption coefficient and decreasing the energy gap, and the activation energy increases as the substrate temperature increasing.

Table(4.6): A.C activation energies for Cd_XSe_{1-X} film at different concentration ,thicknesses ,and substrate temperatures.

Concentration (X)	t (nm)	T_s (K)	E_ω (eV) f (Hz)_			
			10^2	10^3	10^4	10^5
0.1	400	300	-	0.121	0.106	0.102
0.2	400	300	0.124	0.053	0.011	0.071
0.3	200	300	0.206	0.183	0.176	0.167
	300	300	0.144	0.132	0.128	0.125
	400	300	0.062	0.021	0.011	0.005
		348	0.095	0.044	0.014	0.008
		373	0.114	0.049	0.0166	0.0132
		393	0.156	0.117	0.050	0.031
	500	300	0.058	0.047	0.011	0.0096
0.4	400	300	0.087	0.039	0.0075	0.006

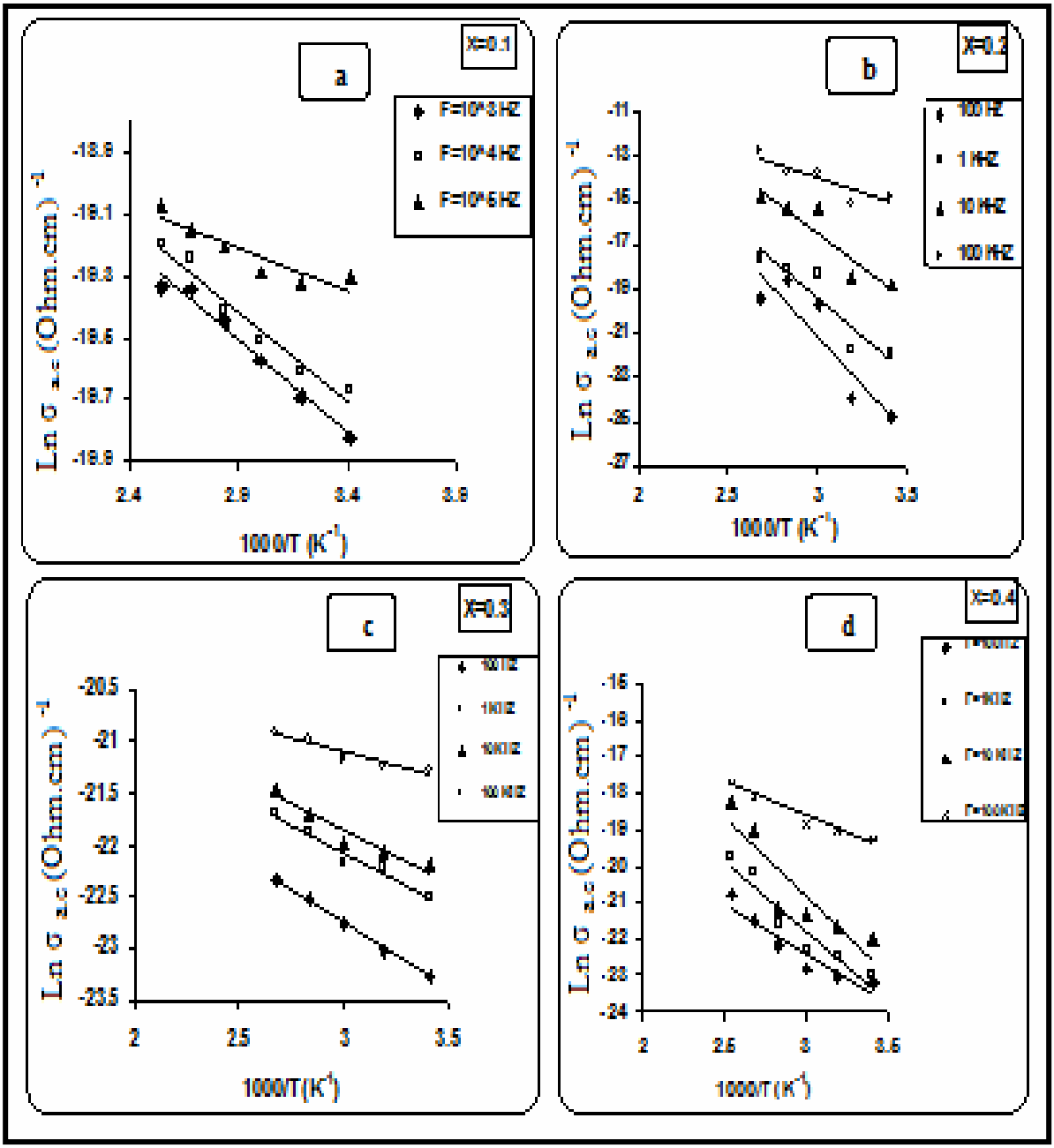

Figure(4.24,a,b,c,d) : ln σ $_{a.c}$ as a function of 1000/T for Cd_XSe_{1-X} with (t=400 nm and T_s=300K) at different concentration and frequencies temperature (a): 0.1 (b): 0.2 (c): 0.3 (d): 0.4 .

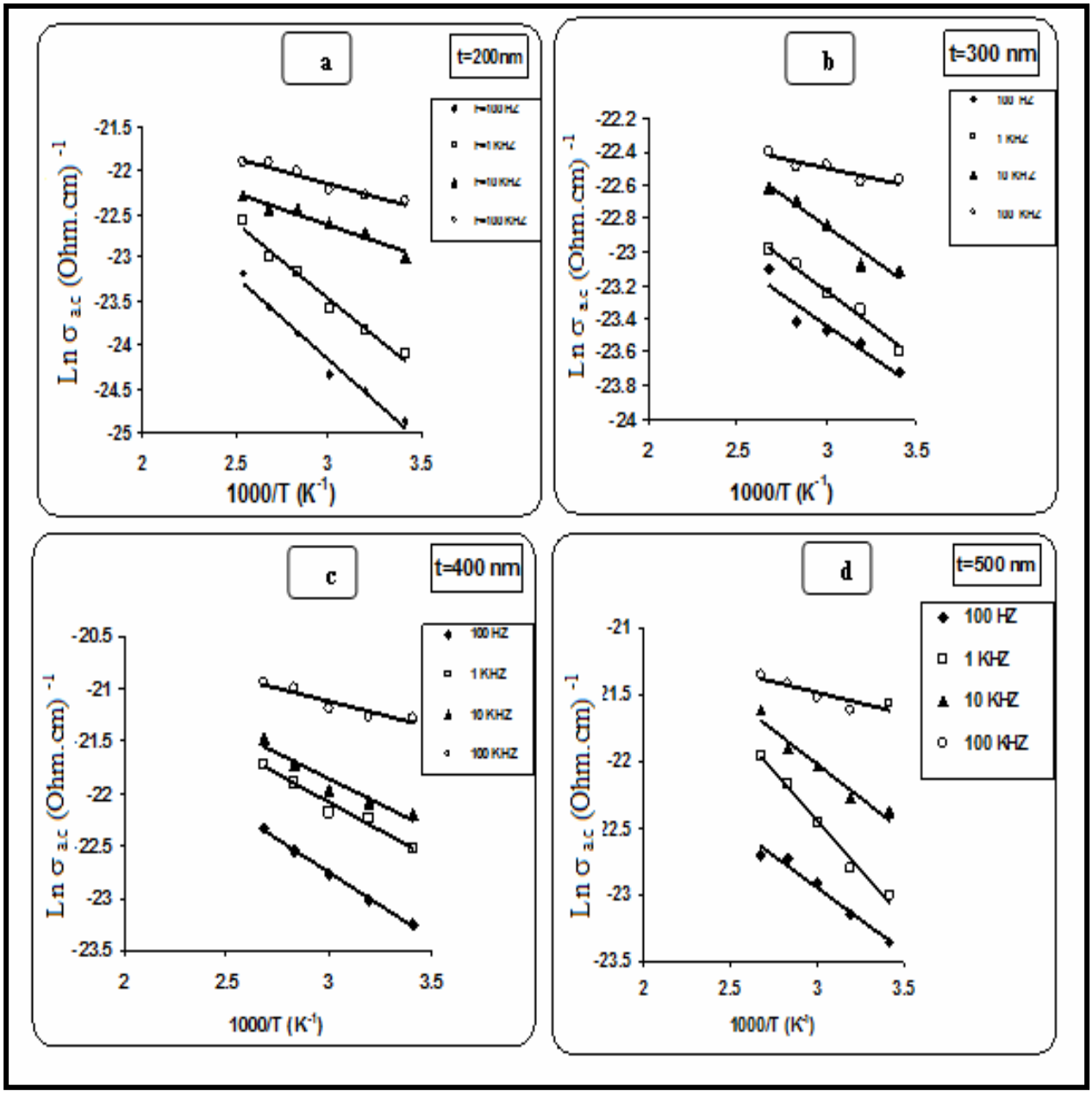

Figure(4.25,a,b,c,d) : ln σ $_{a.c}$ as a function of 1000/T for Cd_XSe_{1-X} with (X=0.3, and T_s=300 K) at different thickness and frequencies (a): 200 nm (b): 300 nm (c): 400 nm (d): 500 nm .

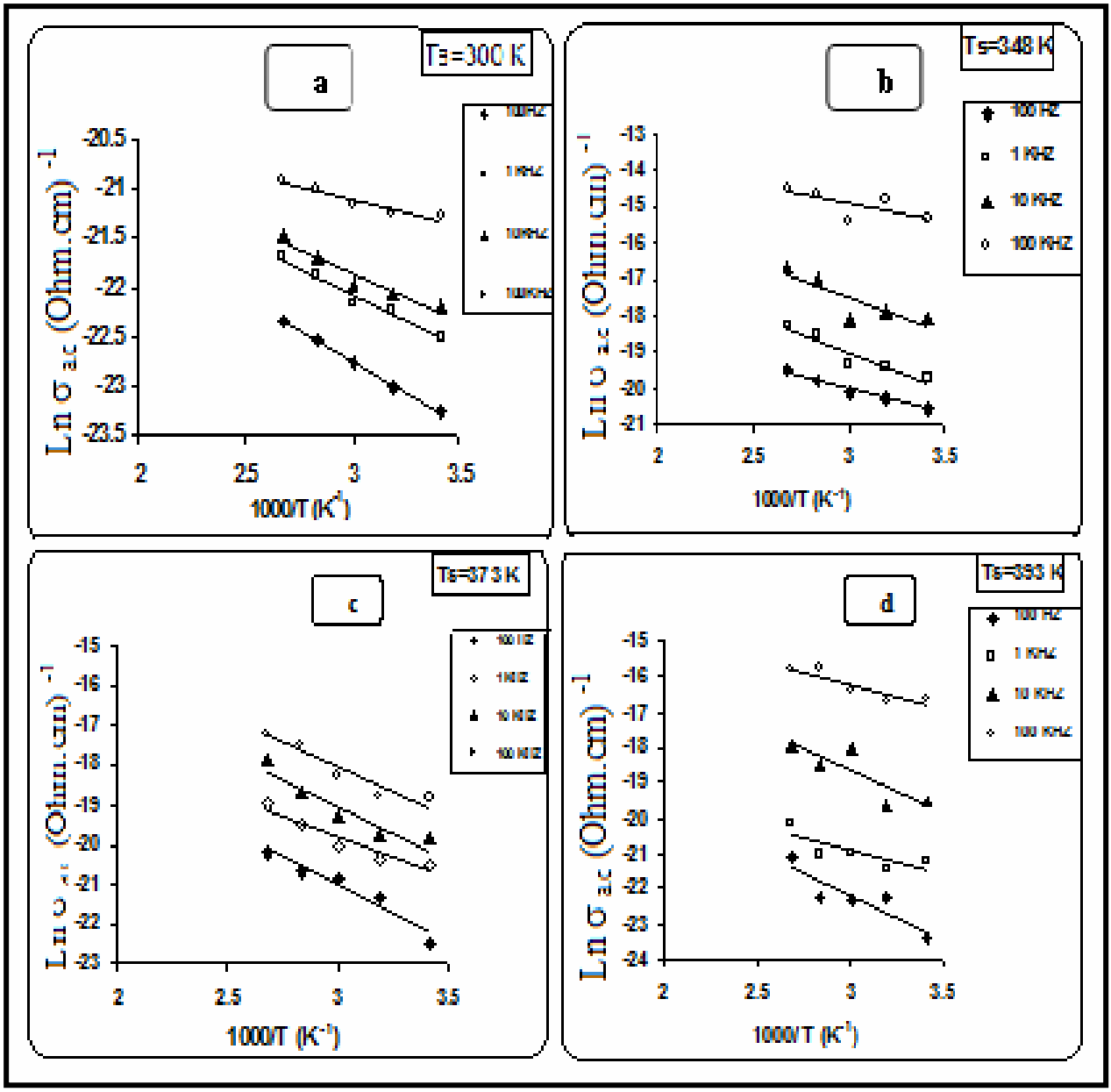

Figure(4.26,a,b,c,d) : ln $\sigma_{a.c}$ as a function of 1000/T for Cd_XSe_{1-X} ,(X=0.4, and t=400nm) at different substrate temperature and frequencies (a): 300 K (b): 348 K(c): 373 K (d): 393 K.

(4-6) Complex permittivity plot (Cole-Cole Diagram) :

The real and imaginary part of dielectric constant calculate from these equations[61] : $\varepsilon_1(\omega)=tC/a\ \varepsilon_0$

$$\varepsilon_2(\omega) = \sigma_{ac}(\omega)/\varepsilon_0\omega$$

Where $\varepsilon_1(\omega)$ is the real part of the complex dielectric (dielectric constant) and $\varepsilon_2(\omega)$ is the imaginary part (Dielectric loss factor) ,Where ε_0 is the permittivity in vacuum, t is the thickness of the samples, a is the electrode area and C is the capacitance of the sample. Representative plots of dielectric constant (ε_1) versus dielectric loss (ε_2) at different conditions [concentration (X), thickness (t), and substrate temperatures (T_s); are shown in figures[4.27,28,29 (a,b,c,d)].

These figures shown a semi- circle diagram, each semi-circle has its center below ε_1-axis . It begins from the origin at the high frequencies and ends at a point on the ε_1-axis at low frequencies .

The intersection of the semi-circle at higher frequencies with ε_1 –axis gives the static dielectric constant (ε_o) (ω=0), and the intersection of the semi-circle at lower frequencies with ε_1-axis gives the optical dielectric constant(ω= higher).The polarizability (α) (dispersion parameter) which calculated according to this relation [$\alpha = \frac{2\theta}{\pi}$] ,where ($\theta$): the angle between ε_1-axis and the diameter of semi-circle .

The Cole-Cole plots are also useful to confirm the distribution of the relaxation time, which can be determined from the relation[62] :

$$\frac{(\varepsilon_s - \varepsilon_o)}{2} = \omega_{\max}\tau$$

where ω_{max} represents the highest frequency and τ is the relaxation time which corresponds to the high value of dielectric loss.

From Table (4.7) we can observed all the dielectric constants which represent the dielectric response for (Cd_XSe_{1-X}) thin film which prepared at different [X=0.1 ,0.2 ,0.3 ,0.4] ; [t=200,300,400,500] nm, and [T_s =300 ,348 ,373 ,393]K. Seen from the Table (4.8) that the results have unstable behavior with different concentration (X), which can be interpreted as a compositional disorder change [63].

The dependence of dielectric parameters on the substrate temperature we seen from the Table (4.7) that (ε_s) increases with substrate temperatures most of this behavior due to the increase in thermal energy will break the intermolecular interaction, resulting in reduction of the values of relaxation time(τ) [70] ,and we observe that (τ) decreasing with increasing (T_s) due to the increasing velocity of the charge carriers; and the disappearance of localized states will increase the scattering factor of charge carriers leading to shorter mean free paths. This result is consistent with previous mentioned data that dc conductivity decreases with T_s , and from figure (4.29,c) we notice that there are two relaxation region on the film which prepared at (T_s=373 K) (i.e: relaxation time distribution had been happened).

Table(4.7):Cole-Cole representation parameters for Cd_XSe_{1-X} thin films.

X	t (nm)	T_s (K)	α	ε_s	$\tau \times 10^{-5}$ (sec)	$\tau_D \times 10^{-5}$ (sec)
0.1	400	300	0.088	5.8	1.9	2.75
0.2	400	300	0.22	5.4	3.9	1.21
0.3	200	300	0.188	1.9	1.48	9.1
	300	300	0.077	1.85	0.73	11.1
	400	300	0.066	3.7	33.8	111
		348	0.111	10	23.5	9.3
		373	0.144 0.077	11 19.5	16.4 13.67	3.36 2.61
		393	0.055	28	8.9	1.11
	500	300	0.055	6.5	5.17	0.45
0.4	400	300	0.122	4.46	27.8	133

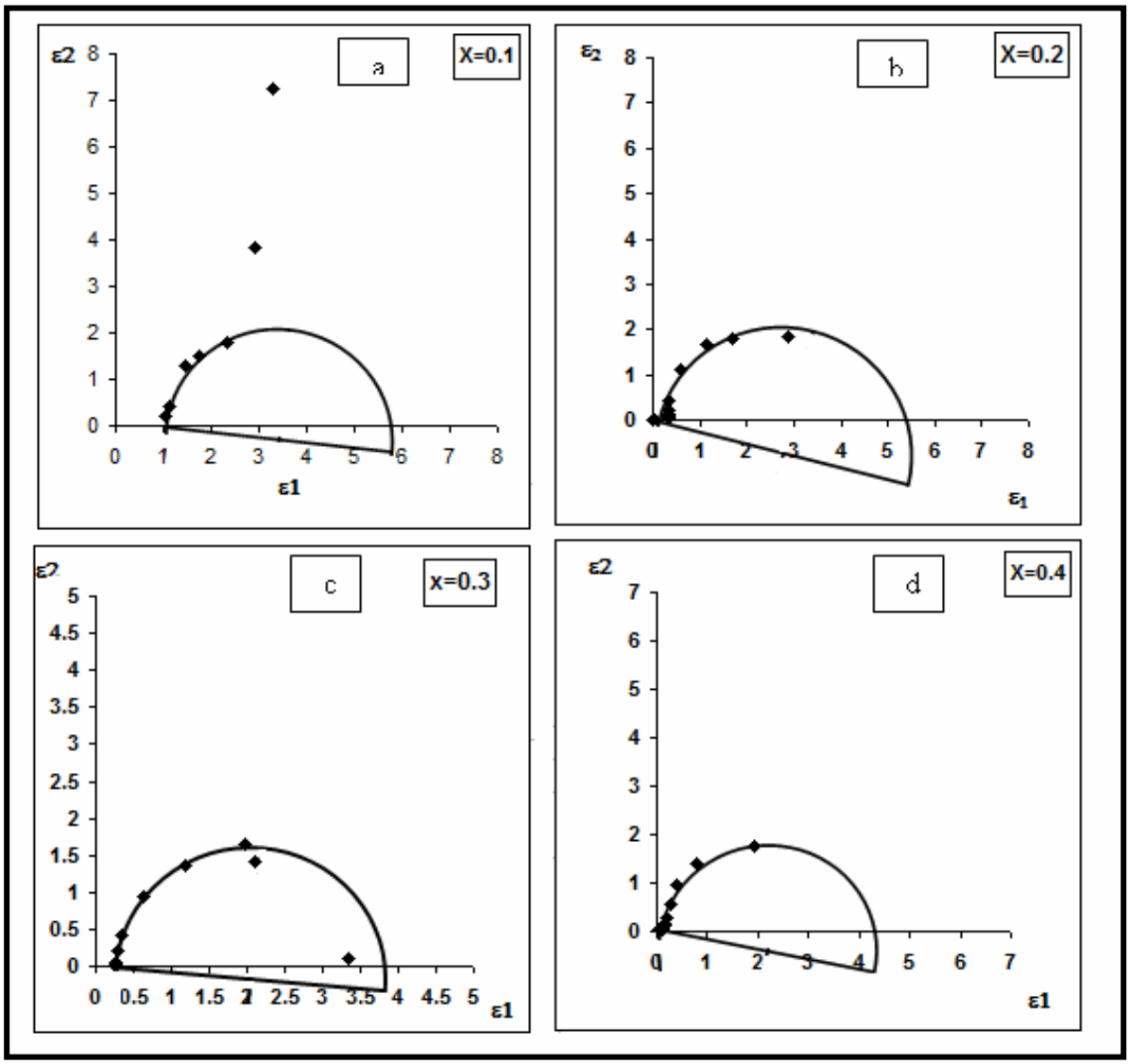

Fig.(4.24) Cole-Cole diagram for Cd_XSe_{1-X} thin film at different concentration (a): 0.1 (b): 0.2 (c): 0.3 (d): 0.4 , and (t=400 nm , T_s=300 K).

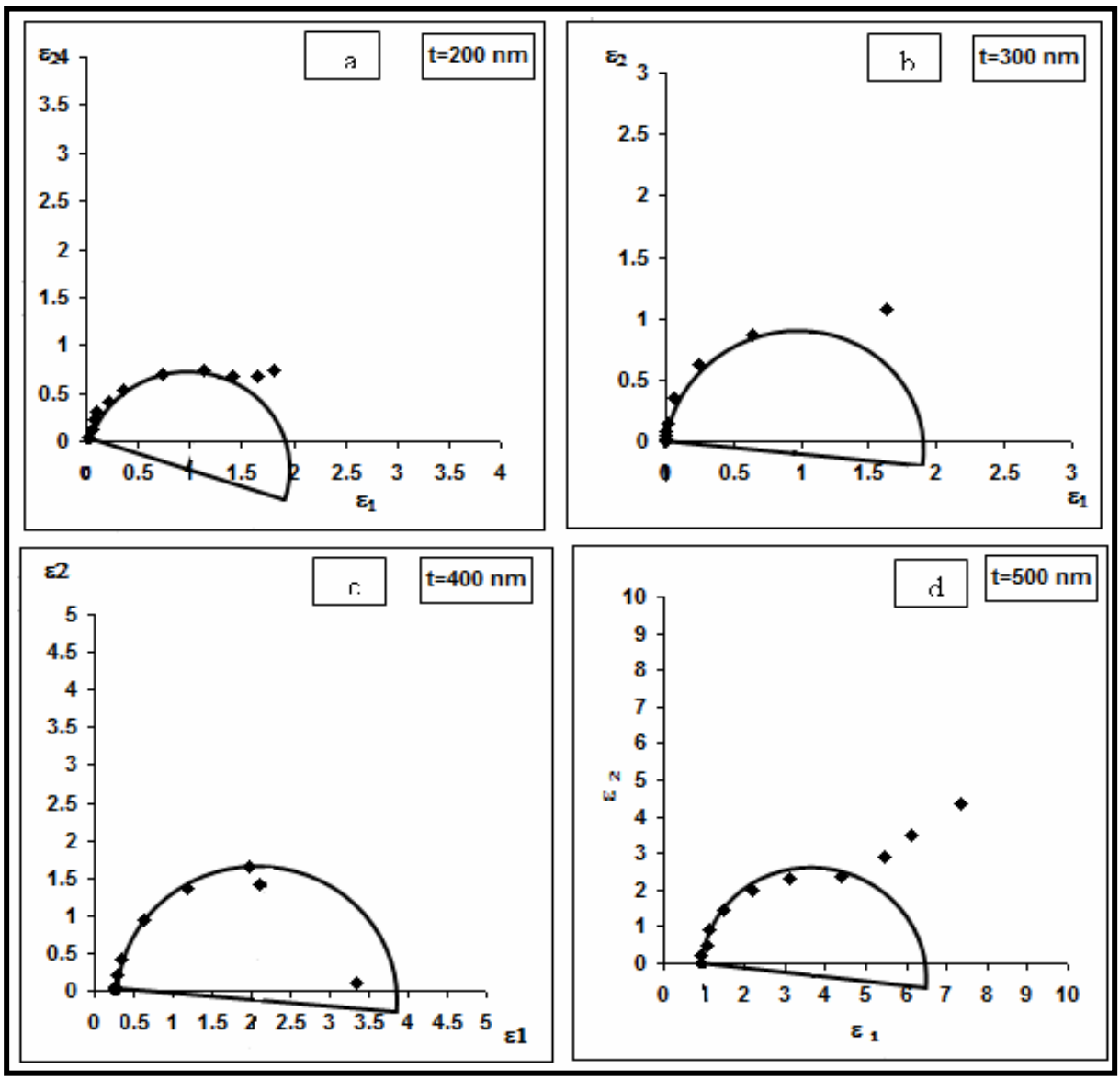

Fig.(4.25) Cole-Cole diagram for Cd_XSe_{1-X} thin film at different thicknesses (a): 200 nm (b): 300 nm (c): 400 nm (d): 500 nm , and (X=0.3 and T_s=300 K).

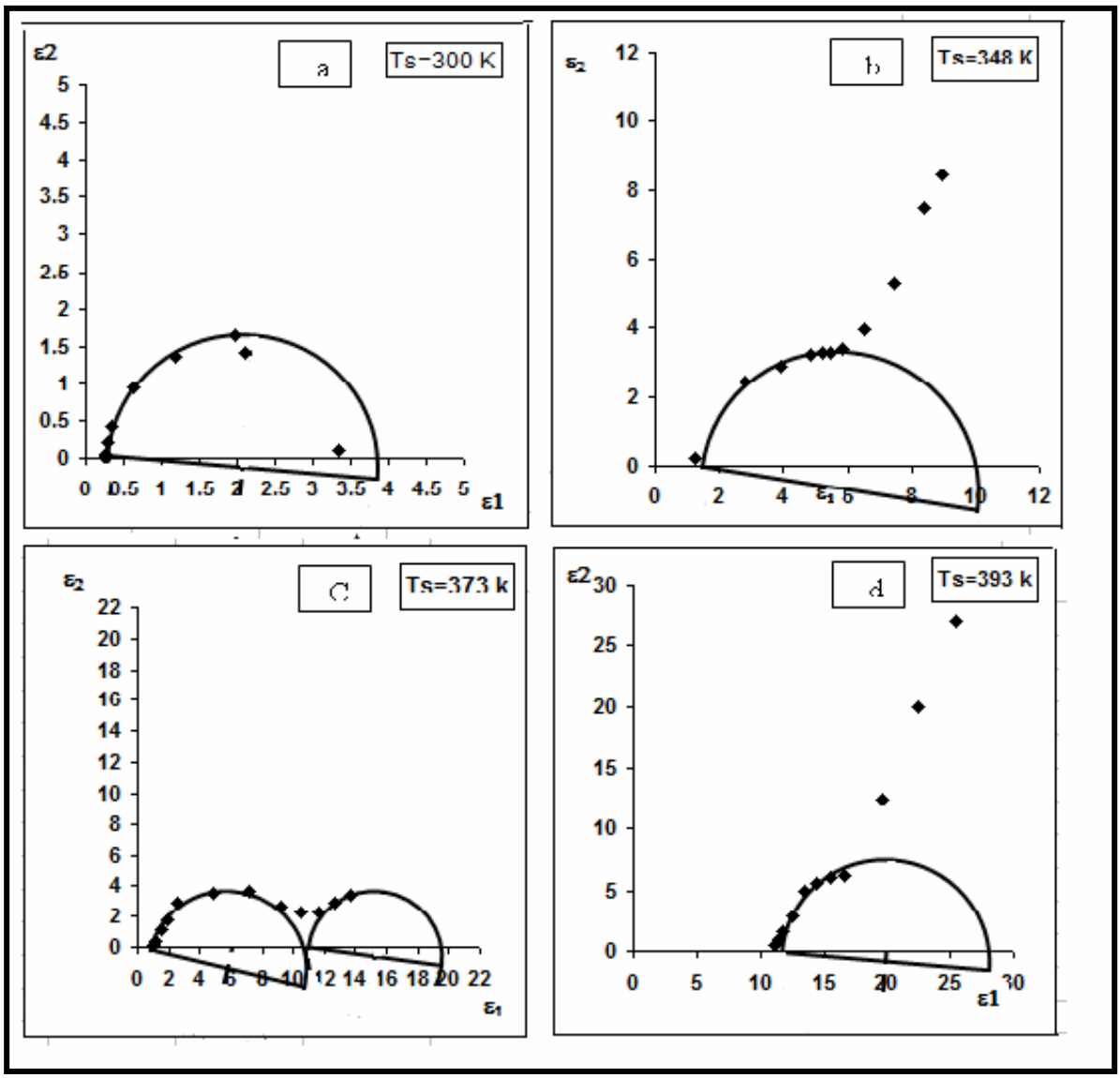

Fig.(4.26) Cole-Cole diagram for Cd_XSe_{1-X} thin film at different substrate temperature (a): 300 K (b): 348 K(c): 373 K (d): 393 K and (X=0.3 and t=400 nm).

Chapter Five

Conclusions

And

suggestions

(5-1) The Conclusions:

The following conclusions can be deduced from this work:

The direct mixing of the elements inside a quartz tube in a vacuum gives a polycrystalline structure with a hexagonal of wurtzite type for a compound at (X=0.2) with mixture of hexagonal and cubic for other compound at (X=0.1,0.3,0.4). The structural properties of Cd_XSe_{1-X} thin film dependent directly by concentration (X), thickness (t), and the substrate temperatures (T_s) was a polycrystalline structure with mixture of hexagonal and cubic phase for all the films except the film at (X=0.2) change the structure to polycrystalline with cubic phase .

The D.C. conductivity for all films increases as the thickness increases, and decreases with increasing the substrate temperature, while it showed irregular behavior with the concentration. There are two transport mechanisms of the charge carriers. In general, the activation energies decrease with increasing the thicknesses, and increasing with increasing the substrate temperature.

The A.C. conductivity measurement showed that the exponent s is a function on the temperature and C.B.H model is the must suitable to interpret our result. From the Cole-Cole diagram we found that the static dielectric constant (ε_s) increasing with increasing the substrate temperature and decreasing in relaxation time with increasing the substrate temperature , and the parameter (α) is less than 1 (i.e $\alpha \approx 0$); the samples shows pure resistance element This means that the film is good to be resistors [64].

Hall measurements confirmed that all the films are (p-type).

(5-2) Suggestions for Future Work:

1. Deposition Cd_XSe_{1-X} films on single-crystalline substrate such as, Nacl , Kcl.
2. Study the surface morphological analysis by using scanning electron microscopy (SEM) technique.
3. Study the electrical properties of Cd_XSe_{1-X} thin film at low temperature.
4. Take the advantage of the results of the study with addition of different materials to manufacture solar cells.

References

References

1- R.W. Berry and P.M. Hall, "*Thin Film Technology*", New York, (1979).

2- K. L. Chopra, "*Thin Film Phenomena*", Mc – Graw Hill, New York, (1969)

3- L. Eckortova, "*Physics of Thin Films* ", (plenum press), (1977).

4- A.H. Anderson, " *Solar cell* " (5), (1982), (234-268).

5- Marshall and A.E.Owen,"phil.Mag.";V.24,(1971) P.1281.

6- S.R.Elliott,"physics of Amorphous Materials",Longman Inc;New York (1984).

7- K.L. Chopra, "Thin Film Device Application", Plenum Press, New York USA (1983).

8- Tribble,"Electrical Engineering Materials and Devices" University of Lowa,(2002).

9- R. A. Smith, "*Semiconductors*", (Cambridge press, 2nd.ed.), (1987

10- Shareef Ahmed Khairi, Hassan Hessian Hassan, "*Semiconductors*", Dar El-Fiker El-Arabi press , Cairo, Egypt, 2008

11-J.S.Blakmore, "Solid state physics",Cambridge Press, 2nd edition(1986).

12-J.Tauce,"Amorphous and Liquid Semiconductors" Plenum Press, London and New York,(1974).

13- R.Pierrent "Semiconductor Fundamentals",2nd ed,ol1Appison.Wesley,(1989).

14-Klug Alexander H.P."X-ray diffraction procedure for polycrystalline and Amorphous material" John Wiely and Sons E.(1974).

15- David Alder, Brain B. Schwartz, Martinc Steele "physical properties of Amorphous materials" Plenum Press New York (1985) (p113).

16- S.M.Sze "physics of semiconductor Devices" 2nd edition Wielly and Sons Inc, N.Y.(1981).

17-B.Ray "II-VI Compounds" 1st edition print in great Britain by Nill and Co-Ltd of Edinburgh (1969).

18-D.S.H.Chan and A.E.Hill , "Thin Solid films",V.35 , P.337, 1976

19-Fantini.M.C.A, J.R.Moro and F.Decker "solar energy matrial" V.17 P.247-255 (1988).

20-Roth.M,"Nuclear instruments and methods in physics Research" V.283 P.291-298 (1989).

21-M.Bouroushian, J.Charoud-Got, Z.Loizos, N.Spyrellis and G.Maurin "Thin solid films", V.381 P.39-47,(2001).

22- D.B.Holt and B.G.Yacobi,"Extended Defects in Semiconductors" ,Cambridge University press ,New Yourk, p.19,(2007).

23-A.Kubovy, I. Hamersky and B.Symersky, "Thin solid films", V.4, P.35-40,(1969).

24- V.Snejdar and J.Jerhot, "Thin solid films", V.11, P.289-298, (1972).

25- Thutupalli GKM and SG.Tomin,"J.Phy.D.App.phys", V.9, P.1639,(1976).

26- Neelkanth G.Dhere, Nalin R.Parikh and Adolpho Ferreira, "Thin solid films", V.44,P.83, (1977).

27- K.N,Sharma and K.Barua, "J.Phy D:Appl.Phys", V.12, P.1729,(1979).

28- S.Uthanna and P..J.Reddy "Phys.stat.sol.", V.65,P.113,(1981).

29- Masahiko Htyngaji and Tado miura TPN.J.Appl.Phys.V24 (1986),N.11, P. 1575

30-F.Raoult, R.Fortin, "Thin solid films"V.182, P.1,(1989).

31- A.Mondal, A.Dahr, S.Chandhuri and A.K.Pal, "Journal of material science", V.25, P.2221-2226, (1990).

32- D.R.Rao and R.Islam, "Thin solid films", V.224, P.191-195, (1993).

33- C.S.Shaharie, D.S.Sutrave & L.P.Deshmukn, "Indian Journal of pure & Applied physics",V.34, P.153-157, (1996).

34- Wafa Abdul-Moeen Makeeha," preparing and studying some properties of CdSe thin films",M.S.C thesis, Al-Muatansiriyah Uni, (1998).

35- Abbas Kamal Hasan,"Dependence of A.C Conductivity for CdSe thin films on the rate of deposition,substrate temperature and frequency".M.SC.thesis, Al-Mustansiriyah Univ,(2001).

36- K.N.Shreekanthan, B.V.Rajendra, V.B.Kasturi and G.K.Shakumar, "Crystall Research technology", V.38, No.1, P30-33, (2003).

37- C.Baban, G.I.Rusu and P.Prepelita, "Journal of optoelectronics and Advanced materials",V.7,No.2,P.817-821, (2005).

38- N.J.Suthan Kissinger, M.Jayachandran, K.Perumal and, C.Sanjeevi Raja, "Indian Academy of sciences".V.30, No.6, P.547-551,(2007).

39-M.Elahi and, N.Ghobadi,"Iranian physical Journal" V.2, No.1, P.27-31, (2008).

40- Haidar Jwad Abdul-Ameer, "Electronic transport mechanism and optical properties of CdSe junction with different substrates",Ph.D ,thesis ,Baghdad Univ.(2009).

41- A.Islam, M.Islam, M.Choudhury, and M.Hossan, "Recent development in condensed matter physics and nuclear science", Rajshahi University, Bangladesh, 28 Oct.-1Nov., (1996).

42- N.F.Mott and Davis, "Electronic process in non-crystalline materials" 2nd ed., Clarendon press, Oxford, (1979).

43- Akira Doi, "J.Appl.Phys."vol.63,(1988),P.(121).

44 – S.R.Elliot"Phil.Mag.B",vol.37,No.5,(1978),P.(553-560).

45- S.R.Elliot, Phil. Mag.B.Vol.38,No.4 (1978).

46- S.R.Elliot "Adv.in Phys."vol.36, (1987),P.(135-218).

47- K.Shimakawa,A.Wataube and K.Hattori”Phil.Mag.B", vol.54 , (1986) , P.(391-414).

48- Izzat.M.Al-Essa"Structural,Optical and electrical properties of a-Si:H" Ph.D. thesis, Baghdad Univ.(1993).

49- M.Pollak and T.H.Gebal "Phys.Rev. " vol.122,(1962),P.(1742).

50- I.G.Austin and N.F. Mott"Adv.Phys." vol.18,(1969)P.(41).

51- M.Pollak "Phil.Mag." vol.23,(1971),P.(519).

52- Georg – Hass, physics of thin films, V11 (1980), this subject writing by A.K.Jonscher.

53- Samiha T. Bishay "Egypt .J.Sol." ,Vol.(23), No.(2), 2000

54-B .K .P .Scaife "principles of dielectrics" Oxford press (1998)

55- A.R.Long“Adv.Phys."vol.31,(1982),P.(533).

56- C.Kittle, "Introduction to Solid State Physics", Eight Ed., John Wiley and Sons, P.416 (2005).

57- V.M. Goldshmidt, "Phys. Rev." 120, P.745, (1960).

58-Izzat M.AL-Essa "Fondazione Giorgio Ronchi" Anno LXIII, N.4, 2008.

59- N.Tigau, V.Civpina, "Journal Of Optoelectronics and advanced materials",V.8, N.1, P. 37-42, (2006).

60-D.P.Padiyan, A.Marikani, and K.R.Murali, "Materials Chemistry and Physics", 78, 355-362, (1972).

61-W.R.Runyan “Semiconductor Measurements and Instrumentation” Texas instruments Incorporated.2nd ed, McGraw-Hill kogausha, Tokyo(1975).

62-A.Abdel Aal "Egypt.J.Solids" Vol.29 , No. 2 , (2006) , p(303-316).

63-M.F.A.Alias, M.N.Makadsi, and Z.M.AL-Ajeli "Turk. J .phys." , Vol.27,(2003),p(133-143).

64- J. Simoockova, P.Miklos ,V .Saly, Acta Physica,VOL.50, No.6, (2000)

الخلاصة

تناولت هذه الرساله دراسه تأثير ظروف التحضير من نسب مختلفه (X) (0.1,0.2,0.3,0.4) و أسماك (t) مختلفه (200-500)nm و درجات حراره اساس (T_s) مختلفه (300-393)K على الخواص التركيبيه و الكهربائيه للأغشيه Cd_XSe_{1-X} الرقيقه المحضره بواسطه تقنيه التبخر الحراري على ارضيات زجاجيه تحت ضغط ($2X10^{-5}$mbar) ومعرفه ميكانيكية الانتقالات الالكترونيه (التوصيليه المستمره و المتناوبه).

تم تحضير سبائك (Cd_XSe_{1-X}) بالنسب المختلفه داخل أنبوبة كوارتز مفرغة من الهواء تم تسخينها الى درجه ألأنصهار وتركها لمده خمس ساعات لضمان تجانس المركب واجراء التبريد البطيء لها الى درجه حراره الغرفه.و تبين من طيف ألأشعه السينيه ان جميع السبائك لها تركيب متعدد التبلور(polycrystalline) بطور سداسي التركيب نوع (Wurtzite) للنسبه(X=0.2) وطور سداسي ومكعب للنسب (X=0.1,0.3,0.4).

كما أظهرت فحوصات حيود ألأشعه السينيه بأن ألأغشيه ألمحضره ولجميع النسب عند سمك (400nm) وعند درجه حراره الغرفه كانت متعدده التبلور(polycrystalline) و ذات تركيب مختلط سداسي ومكعب عند (X=0.1,0.3,0.4) وعند نفس ظروف التحضيركانت متعدده التبلور(polycrystalline) بطورمكعب وبأتجاه مفضل (111) للنسبه(X=0.2) و كانت ألأغشيه ألمحضره بنسبه(0.3) وعند درجه حراره الغرفه وبأسماك مختلفه متعدده التبلور(polycrystalline) ذات تركيب مختلط سداسي ومكعب الطورو بألأتجاه المفضل(111) ،وعند نفس النسبه وبسمك (400nm) وعند زياده درجه حراره ألأساس كانت ألأغشيه متعدده التبلور(polycrystalline) وذات تركيب سداسي ومكعب و الاتجاه المفضل (111) وكانت هناك زياده في نسبه السيلينيوم (Se) في تلك ألأغشيه.

ألتوصيليه الكهربائيه المستمره اظهرت تصرف غير واضح بزياده النسب وذلك بسبب تغير التركيب،كما ان التوصيليه كانت تزداد بزياده السمك ولوحظ حاله معاكسه عند زياده درجه حراره ألأساس. كما لوحظ ان هناك منطقتا تنشيط لجميع ألأغشيه المحضره.

أما بالنسبه للتوصيليه الكهربائيه المتناوبه لجميع ألاغشيه المحضره ومن خلال دراسه تغاير كل من التوصيليه المتناوبه والعامل ألأسي (S) مع التردد الزاوي ودرجه الحراره تبين ان انسب نموذج يفسر النتائج العمليه هو نموذج تنطط الحاجز المرتبط (CBH)

وكذلك بواسطه مخطط كول-كول تم حساب كل من زمن الأسترخاء (τ)و(τ_D) لنموذج ديباي المثالي والغير مثالي على التوالي ،الاستقطابيه(α) وثابت العزل الاستاتيكي (ε_s) ولوحظ زياده في ثابت العزل الاستاتيكي من 3.7 الى 28 ونقصان بزمن الاسترخاء مع زياده درجه حراره ألأساس من K (300 -393) .

وبينت قياسات تجربه هول ان جميع الاغشيه المحضره كانت من نوع (p) .

جمهورية العراق
وزارة التعليم العالي والبحث العلمي
جامعة النهرين/ كلية العلوم
قسم الفيزياء

الخواص التركيبيه و ميكانيكيه ألتوصيل المستمر و المتناوب للأغشيه الرقيقه Cd_XSe_{1-X} المحضره بطريقه التبخير الحراري

رسالة مقدمة ألى
قسم الفيزياء/كلية العلوم/جامعة النهرين
كجزء من متطلبات نيل درجة ماجستير في الفيزياء

من قبل
صبا نشأت سعيد ألخفاجي
بكالوريوس 2005

بأشراف

أ.د.عزت محمود العيسى ***م.د. طالب سلوم حمادي***